UNIVERSITÄTSKLINIKUM HAMBURG-EPPENDORF

Institut für Experimentelle Immunologie und Hepatologie

Prof. Dr. rer. nat. Gisa Tiegs

Antigen Cross-Presentation by Murine Proximal Tubular Epithelial Cells Induces Cytotoxic and Inflammatory $CD8^+$ T Cells

Dissertation

zur Erlangung des Grades eines Doktors der Medizin

an der Medizinischen Fakultät der Universität Hamburg.

vorgelegt von:

Alexandra Linke

aus Buxtehude

Hamburg 2022

Angenommen von der

Medizinischen Fakultät der Universität Hamburg am: 28.02.2023

Veröffentlicht mit Genehmigung der

Medizinischen Fakultät der Universität Hamburg.

Prüfungsausschuss, der/die Vorsitzende: Prof. Dr. Ulf Panzer

Prüfungsausschuss, zweite/r Gutachter/in: Prof. Dr. Gisa Tiegs

Gewidmet meiner Familie

Content

1 Original version of the publication including supplemental data

The following pages contain the published manuscript including supplemental data.

cells

MDPI

Article

Antigen Cross-Presentation by Murine Proximal Tubular Epithelial Cells Induces Cytotoxic and Inflammatory CD8$^+$ T Cells

Alexandra Linke [1,†], Hakan Cicek [1,†], Anne Müller [1,2], Catherine Meyer-Schwesinger [3], Simon Melderis [2,4], Thorsten Wiech [5], Claudia Wegscheid [1], Julius Ridder [1], Oliver M. Steinmetz [2,4], Linda Diehl [1,2], Gisa Tiegs [1,2] and Katrin Neumann [1,2,*]

[1] Institute of Experimental Immunology and Hepatology, University Medical Center Hamburg-Eppendorf, 20246 Hamburg, Germany; alexandra_linke@web.de (A.L.); hakan.cicek@stud.uke.uni-hamburg.de (H.C.); anne.mueller1@uke.de (A.M.); c.wegscheid@web.de (C.W.); julius.ridder4u@gmail.com (J.R.); li.diehl@uke.de (L.D.); g.tiegs@uke.de (G.T.)
[2] Hamburg Center for Translational Immunology, University Medical Center Hamburg-Eppendorf, 20246 Hamburg, Germany; s.melderis@uke.de (S.M.); osteinmetz@uke.de (O.M.S.)
[3] Institute of Cellular and Integrative Physiology, University Medical Center Hamburg-Eppendorf, 20246 Hamburg, Germany; cmeyer-schwesinger@uke.de
[4] III. Medical Clinic, University Medical Center Hamburg-Eppendorf, 20246 Hamburg, Germany
[5] Institute of Pathology, University Medical Center Hamburg-Eppendorf, 20246 Hamburg, Germany; t.wiech@uke.de
* Correspondence: kat.neumann@uke.de
† These authors contributed equally to this work.

check for updates

Citation: Linke, A.; Cicek, H.; Müller, A.; Meyer-Schwesinger, C.; Melderis, S.; Wiech, T.; Wegscheid, C.; Ridder, J.; Steinmetz, O.M.; Diehl, L.; et al. Antigen Cross-Presentation by Murine Proximal Tubular Epithelial Cells Induces Cytotoxic and Inflammatory CD8$^+$ T Cells. *Cells* **2022**, *11*, 1510. https://doi.org/10.3390/cells11091510

Academic Editor: Kathrin Eller

Received: 8 April 2022
Accepted: 28 April 2022
Published: 30 April 2022

Publisher's Note: MDPI stays neutral with regard to jurisdictional claims in published maps and institutional affiliations.

Abstract: Immune-mediated glomerular diseases are characterized by infiltration of T cells, which accumulate in the periglomerular space and tubulointerstitium in close contact to proximal and distal tubuli. Recent studies described proximal tubular epithelial cells (PTECs) as renal non-professional antigen-presenting cells that stimulate CD4$^+$ T-cell activation. Whether PTECs have the potential to induce activation of CD8$^+$ T cells is less clear. In this study, we aimed to investigate the capacity of PTECs for antigen cross-presentation thereby modulating CD8$^+$ T-cell responses. We showed that PTECs expressed proteins associated with cross-presentation, internalized soluble antigen via mannose receptor-mediated endocytosis, and generated antigenic peptides by proteasomal degradation. PTECs induced an antigen-dependent CD8$^+$ T-cell activation in the presence of soluble antigen in vitro. PTEC-activated CD8$^+$ T cells expressed granzyme B, and exerted a cytotoxic function by killing target cells. In murine lupus nephritis, CD8$^+$ T cells localized in close contact to proximal tubuli. We determined enhanced apoptosis in tubular cells and particularly PTECs up-regulated expression of cleaved caspase-3. Interestingly, induction of apoptosis in the inflamed kidney was reduced in the absence of CD8$^+$ T cells. Thus, PTECs have the capacity for antigen cross-presentation thereby inducing cytotoxic CD8$^+$ T cells in vitro, which may contribute to the pathology of immune-mediated glomerulonephritis.

Keywords: proximal tubular epithelial cells; antigen cross-presentation; cytotoxic CD8$^+$ T cells; apoptosis; lupus nephritis

1. Introduction

Immune-mediated glomerular diseases are characterized by renal infiltration of T cells that localize in the tubulointerstitium in close contact to tubular epithelial cells. Interactions between lymphocytes and renal epithelial cell populations have been suggested to contribute to kidney disease pathology [1,2]. Proximal tubular epithelial cells (PTECs) have been described as a population of renal non-professional antigen-presenting cells (APCs),

which induce antigen-specific $CD4^+$ T-cell activation [3,4] and inflammatory cytokine expression [4]. PTECs are characterized by a low expression of major histocompatibility complex class (MHC)-II in homeostasis [3,5,6], which is upregulated in kidney diseases [5,7–9]. They present antigen via MHC-II [3], and express co-stimulatory molecules [4,10,11] thereby facilitating $CD4^+$ T-cell activation.

Cross-presentation is a process by which exogenous soluble antigens are presented through APCs on MHC-I to activate $CD8^+$ T cells [12–14]. The cross-presentation pathway plays a key role in $CD8^+$ T cell-mediated immunity to certain infections [15], tumors [16], and organ transplants [17]. It also contributes to autoimmune diseases where cross-presentation of self-antigens triggers autoimmunity [18]. Initially thought to be restricted to professional APCs such as dendritic cells (DCs) [19], cross-presentation is also efficiently carried out by liver sinusoidal endothelial cells (LSECs), a population of non-professional APCs in the liver [20,21]. Interestingly, antigen cross-presentation by LSECs induces $CD8^+$ T-cell tolerance rather than immunity [22–24].

The major pathway for antigen cross-presentation is the endosome-to-cytosol pathway [25]. The mannose receptor (MR) has been implicated in the uptake of soluble antigen and its endosomal localization [26,27]. Internalized antigens are transported from endosomes into the cytosol for proteasomal degradation. Antigen translocation into the cytosol involves the valosin-containing protein (VCP), an ATPase that provides energy for antigen transport across endosomal membranes [28]. The trimeric translocon Sec61 has been suggested as an endosomal transmembrane pore complex crucial for antigen translocation [29,30]. The immunoproteasome and its specific subunit large multifunctional peptidase (LMP7) have been implicated in the processing of antigenic peptides for presentation on MHC-I [31,32]. Proteasome-derived peptides are transported by the transporter associated with antigen processing (TAP1) and TAP2 from the cytosol back into endosomes [33], where they are loaded onto MHC-I. Therefore, peptides are trimmed into suited sizes via the endosomal leucyl-cystinyl aminopeptidase (LNPEP) [34]. To avoid pH-dependent activation of proteases leading to impaired antigen cross-presentation, alkalization of endosomes is mediated by the NADPH oxidase (NOX)2 [35,36]. Subsequently, MHC-I/peptide complexes are transported to the cell surface for presentation to $CD8^+$ T cells.

Whether PTECs have the capacity to activate $CD8^+$ T cells via antigen cross-presentation and what phenotype PTECs induce in $CD8^+$ T cells is not known so far. Identifying the nature of PTEC-induced $CD8^+$ T-cell responses may help to understand the impact of renal epithelial cell-mediated modulation of infiltrating T cells on the pathogenesis of immune-mediated glomerulonephritis (GN). In this study, we describe the potential of PTECs for antigen cross-presentation in vitro, identify pathways of soluble antigen internalization and processing, determine the phenotype of PTEC-activated $CD8^+$ T cells in co-culture, and analyze the capacity of PTEC-activated $CD8^+$ T cells to induce apoptotic cell death. We further assess the impact of $CD8^+$ T cells on the induction of apoptosis in renal tissue in murine lupus nephritis.

2. Material and Methods

2.1. Animals

Mice of the following types were bred in the animal facility of the University Medical Center Hamburg-Eppendorf (UKE; Hamburg, Germany): C57BL/6 wild-type (WT), *Cd8a*$^{-/-/-}$, and C57BL/6-Tg(TcraTcrb)1100Mjb/Crl (OT-I). A selection of OT-I mice were kindly provided by Dr. Dorothee Schwinge and Prof. Hans-Willi Mittrücker (all UKE, Hamburg, Germany). The MRL/MpJ (MRL) and the MRL/MpJ-*Fas*^{lpr}/J (MRL-*lpr*) mice were purchased at the Jackson Laboratory (Bar Harbor, ME). Mice were bred according to the Federation of European Laboratory Animal Science Association guidelines, and they were maintained under specific-pathogen-free conditions. All mouse experiments were approved by the Behörde für Justiz und Verbraucherschutz (Hamburg, Germany; approval codes: N57/19, ORG 960, and ORG 1032), and they were carried out according

to the current existing guidelines on mouse experimentation. All efforts were made to minimize suffering.

2.2. Animal Treatment

The WT mice and the *Cd8a*$^{-/-}$ mice received a single intraperitoneal injection of 500 µL pristane oil (2,6,10,14-tetramethylpentadecane; Sigma-Aldrich, St. Louis, MO, USA) to induce lupus nephritis, and were analyzed 9 months later.

2.3. Urine Analysis

One day before the final analysis, mice were housed in metabolic cages for urine collection. Albumin levels were determined by ELISA (Mice-Albumin Kit; Bethyl, Montgomery, TX). Creatinine levels were measured with the COBAS INTEGRA Creatinine Jaffé Gen.2 Kit (Roche Diagnostics, Indianapolis, IN, USA). The albumin-to-creatinine ratio was calculated to assess the severity of proteinuria.

2.4. Histological Analyses

To identify CD8$^+$ CD3$^+$ T cells in renal tissue, CD8 and CD3 staining was performed in serial sections. Therefore, 2 µm paraffin-embedded kidney sections were stained with anti-CD3 (polyclonal, Agilent Technologies, Santa Clara, CA, USA) or with anti-CD8 (D4W2Z; Cell Signaling Technology, Danvers, MA, USA) antibodies. Prior to CD8 staining, heat-induced antigen retrieval was achieved by using a citrate buffer (pH 6). A horseradish peroxidase (HRP)-conjugated anti-rabbit antibody (ThermoFisher Scientific, Waltham, MA, USA) was used as a secondary antibody. The DAB+ Substrate Chromogen System (Agilent Technologies) was used for antigen detection. Prior to CD3 staining, heat-induced antigen retrieval was done by using the Dako Target Retrieval Solution (Agilent Technologies). For antigen detection, New Fuchsin (Merck, Darmstadt, Germany) and the ZytoChem-Plus AP Polymer-Kit (Zytomed Systems, Berlin, Germany) were used, containing an alkaline phosphatase-conjugated anti-rabbit secondary antibody. To assess the number and the localization of CD8$^+$ T cells, kidney sections were scanned using the Zeiss Axioscan 7 (Carl Zeiss, Jena, Germany), and they were analyzed by ZEN lite software (Carl Zeiss). Five corresponding high power fields (hpf) were randomly defined in the cortices of each serial kidney section. Overlapping CD3 and CD8 staining marked CD8$^+$ T cells.

For TUNEL staining, 3 µm paraffin-embedded kidney sections were prepared. The TUNEL assay was performed with the TACS Blue Label In Situ Apoptosis Detection Kit (R&D Systems, Minneapolis, MN) according to the manufacturer's manual. To stain cleaved caspase-3, 2 µm paraffin-embedded kidney sections were incubated with an anti-cleaved caspase-3 antibody (ThermoFisher Scientific). Antigen retrieval was performed in Dako Target Retrieval Solution (Agilent Technologies). After incubation with goat anti-rabbit-HRP secondary antibody (ThermoFisher Scientific), kidney sections were stained with DAB+ substrate (Agilent Technologies). The evaluation was carried out by counting positive events in three random areas (each 125 µm^2) located in renal cortex, from which the mean value was calculated.

Periodic acid-Schiff (PAS) staining was done with 1.5 µm paraffin-embedded kidney sections to assess disease-related pathological changes. The severity of lupus nephritis in MRL-*lpr* and MRL mice was evaluated according to the modified National Institute of Health activity and chronicity indices by a renal pathologist in a blinded manner. The renal activity score comprised glomerular proliferation, leucocyte exudation, karyorrhexis/fibrinoid necrosis (×2), cellular crescents (×2), hyaline deposits and interstitial inflammation [37]. Glomerular abnormalities in pristane-treated mice were determined in a minimum of 50 glomeruli per mouse in a blinded manner. These included glomerular hypercellularity, crescent formation, fibrinoid necrosis, segmental proliferation, hyalinosis and capillary wall thickening [38]. Glomeruli were scored as severely abnormal if they showed intra and/or extra-capillary proliferation or crescents. Glomeruli were scored as

abnormal if they showed mesangial proliferation and/or increased mesangial deposition of PAS-positive material or if they fulfilled criteria for severely abnormal glomeruli.

2.5. Isolation and Culture of PTECs

Kidneys were harvested from WT mice. Renal medulla and adrenal structures were removed and the remaining cortices were finely minced. Renal cortex tissue was digested in DMEM/F-12/GlutaMAX™ medium (ThermoFisher Scientific), containing 0.25% BSA (Serva Electrophoresis GmbH, Heidelberg, Germany) and 0.01% collagenase from *clostridium histolyticum* (Sigma Aldrich, St. Louis, MO, USA) at 37 °C for 17 min. Thereafter, renal tissue was passed through a 250 µm sieve. PTECs were separated from other cortical cells by Percoll density gradient centrifugation, using a solution that contained 45% Percoll (GE Healthcare Life Sciences, Chicago, IL, USA) and 55% 2× PBS-glucose as described previously [4,39]. After gradient centrifugation, PTECs were harvested from the lowest interphase and cultured in DMEM/F12 media supplemented with 1% FCS, 1× I/T/S (mixture of insulin, transferrin, sodium selenite), 50 nM hydrocortisone, 5 nM T_3, 5 nM epidermal growth factor (all Sigma Aldrich), and 1% penicillin/streptomycin (ThermoFisher Scientific) for 5 days to form a monolayer. PTECs were incubated with Alexa Fluor 647-conjugated ovalbumin (OVA; 10 µg/mL; ThermoFisher Scientific) at 37 °C or 4 °C. PTECs were pre-treated with chlorpromazine (30 µM, [40]), mannan (3 mg/mL [26]) or D-galactose (0.125 M [41]; all Sigma-Aldrich) at 37 °C for 1 h before incubation with Alexa Fluor 647-labelled OVA for another hour.

2.6. Isolation and Culture of LSECs

Livers of WT mice were perfused with 0.05% GBSS/collagenase (from *clostridium histolyticum*; Sigma Aldrich) solution, removed, and digested in GBSS/collagenase at 37 °C for 20 min. After filtration through a steel mesh, liver cells were washed twice with GBSS. Non-parenchymal cells were removed by density gradient centrifugation, using a 30% Nycodenz solution (Progen Biotechnik, Heidelberg, Germany). By magnetic-activated cell sorting (MACS), $CD146^+$ LSECs were isolated using CD146 MicroBeads (Miltenyi Biotec, Bergisch Gladbach, Germany). Then, LSECs were seeded onto collagen-coated 24-well plates in DMEM (high glucose) supplemented with 8% FCS (Sigma Aldrich), 2% L-glutamine (Life Technologies, Carlsbad, CA, USA), and 1% penicillin/streptomycin (ThermoFisher Scientific) for 2 days to form a monolayer.

2.7. Generation of Bone Marrow-Derived DCs (BMDCs)

Bone marrow cells were isolated from femur and tibia of WT mice. After erythrocyte lysis through NH_4Cl, 1×10^6 cells were seeded in a petri dish in the presence of GM-CSF (10 ng/mL; PeproTech, Rocky Hill, NJ, USA) for 7–10 days. Thereafter, $CD11c^+$ BMDCs were isolated by MACS using CD11c MicroBeads (Miltenyi Biotec).

2.8. Isolation of $CD8^+$ T Cells and Splenic DCs

From the spleens and the lymph nodes of OT-I mice, OVA-specific $CD8^+$ T cells were isolated; DCs were isolated from the spleens of WT mice. Tissue was passed through 70 µm nylon meshes prior to erythrocyte lysis using NH_4Cl. Thereafter, cells were incubated with anti-CD16/32 antibody solution. Using the $CD8^+$ T cell Isolation Kit (Miltenyi Biotec) according to the manufacturer's instructions, $CD8^+$ T cells were enriched by MACS. Subsequently, $CD8^+$ $CD25^-$ T cells were purely isolated by fluorescence-activated cell sorting (FACS). Using CD11c Microbeads, $CD11c^+$ DCs were isolated by MACS.

2.9. Isolation of Renal Cells

Murine kidneys were harvested, finely minced, and digested for 40 min at 37 °C with 0.4 mg/mL collagenase D and 0.01 mg/mL DNase I (both Roche). Single cell suspensions were achieved by using the gentleMACS Dissociator (Miltenyi Biotec). Cell suspensions

were subjected to a density gradient centrifugation, using a 37% Percoll solution (GE Healthcare Life Sciences) to enrich renal leukocytes. Erythrocytes were lysed with NH_4Cl.

2.10. Co-Culture Experiments

For 2.5 or 5 days, OVA-specific $CD8^+$ $CD25^-$ T cells were co-cultured with PTECs, splenic DCs, or LSECs in the presence or the absence of peptide-free OVA protein (500 µg/mL). Peptide-free OVA protein was generated using Amicon Ultra-15 centrifugal filter devices (Merck), according to the manufacturer's instruction. For immunoproteasome inhibition, PTECs were pre-incubated with ONX 0914 (0.1 µM; Cayman Chemical, Ann Arbor, MI) for four hours. All PTECs were thoroughly washed before co-culture with $CD8^+$ T cells in the presence and the absence of OVA for 1.5 days.

2.11. Flow Cytometry

The $CD8^+$ T cells from co-cultures and renal leukocytes were re-stimulated with phorbol myristate acetate (10 ng/mL) and ionomycin (250 ng/mL) for 4 h with the addition of brefeldin A (1 µg/mL; all Sigma Aldrich) and monensin (BioLegend, San Diego, CA, USA) after 30 min. The anti-CD107a antibody (1D4B; FITC; BioLegend) was added to the restimulation medium. Cells were incubated with anti-CD16/32 antibody solution (93; BioLegend, San Diego, CA, USA) to prevent unspecific antibody binding. LIVE/DEAD Fixable Staining Kits (ThermoFisher Scientific) were used to exclude dead cells. Cells were surface-stained with fluorochrome-labeled antibodies specific to T-cell receptor (TCR)β (H57-597; FITC), CD8a (53-6.7; V500), CD25 (PC61; BV421), CD44 (IM7; BV785), and PD-1 (HA2-7B1; APC; all Biolegend). After fixation and permeabilization (Foxp3 Transcription Factor Staining Buffer Set; ThermoFisher Scientific), $CD8^+$ T cells were stained with antibodies specific to Ki-67 (REA183; FITC), granzyme B (GB11; Pacific Blue), interferon (IFN)γ (XMG1.2; PE- Texas Red), or interleukin (IL)-17A (TC11-18H10.1; PerCP; all Biolegend). To determine cytokine levels in culture supernatants via flow cytometry, the LEGENDplex MU Th Cytokine Panel (12-plex, Biolegend) was used.

2.12. Cytotoxicity Assay

As P815 mastocytoma cells are well described target cells for cytotoxic T cells [42], they were therefore used in the cytotoxicity assay. In a target/effector-cell ratio of 1:6 for 4 h, 1×10^5 P815 cells were cultured with PTEC-activated $CD8^+$ T cells or the respective controls. Cells were stained for CD8 (53-6.7; BV785; BioLegend) to distinguish $CD8^-$ P815 cells from $CD8^+$ T cells. For dead cell discrimination, cells were stained with 7-amino-actinomycin D (7-AAD; PerCP; Biolegend), which binds to the DNA of damaged and dead cells, and it is excluded by intact cells. The staining of CD8 and 7-AAD was done 15 min before data acquisition without cell washing.

2.13. Quantitative Real-Time RT- PCR Analysis

Total RNA was isolated from cultured PTECs, BMDCs, and LSECs using Trizol reagent (ThermoFisher Scientific). The RNA was subjected to DNase (ThermoFisher Scientific) digestion to remove contaminating genomic DNA. The RNA was transcribed into cDNA using the Verso cDNA Synthesis Kit (Life Technologies) on a MyCycler thermal cycler (BioRad, München, Germany). A quantitative RT-PCR was performed using the Absolute qPCR SYBR Green Mix (ThermoFisher Scientific). The relative mRNA levels were calculated using the ΔΔCT method after normalization to the reference gene β-actin. Exon-spanning primers were obtained from Metabion (Martinsried, Germany). Primer sequences are listed in Supplemental Table S1.

2.14. Western Blot Analysis

Cultured PTECs, BMDCs, or LSECs were incubated in a lysis solution containing 1% Triton X-100 (Sigma Aldrich). To prevent proteolytic degradation, incubation was done in the presence of the protease and the phosphatase inhibitors EDTA (5 mM), PMSF (1 mM),

aprotinin, sodium pyrophosphate (10 mM), beta-glycerophosphate (10 mM), sodium orthovanadate (1 mM), sodium pervanadate (0.1 mM), and sodium fluoride (10 mM). Protein concentrations were determined with the Bradford assay. Equal protein levels were used and applied to precast NuPAGE Bis-Tris Gels with a polyacrylamide concentration of 4–12% (ThermoFisher Scientific) for protein separation. Proteins were transferred to a nitrocellulose membrane by tank blotting. Membranes were incubated with anti-TAP1, anti-SEC61A1, anti-NOX2, anti-LNPEP, and anti-VCP (all polyclonal; ThermoFisher Scientific), or with anti-MMR/CD206 (polyclonal, R&D Systems) antibodies. The secondary anti-rabbit or anti-goat antibodies were conjugated to horseradish peroxidase, and binding was visualized by chemiluminescence (ThermoFisher Scientific). To detect the reference protein GAPDH, blots were stripped and incubated with anti-GAPDH (6C5cc; HyTest, Turku, Finland) antibody. To perform a densitometric analysis, blots were analyzed with the Image Lab software (Bio-Rad, Feldkirchen, Germany). Signal intensities of the analyzed proteins were normalized to the reference protein GAPDH.

2.15. Proteasomal Subunit Activity Measurement

Shock frozen pellets of PTECs pre-treated with ONX 0914 (0.1 µM) for 4 h or of rat hybridoma assay control cells were re-suspended in 12 µL TSDG buffer (10 mM Tris-HCl pH 7.5, 10 mM NaCl, 25 mM KCl, 1 mM $MgCl_2$, 0.1 mM EDTA, 1 mM DTT, 2 mM ATP, 10% glycerol), and lysed by 7 freeze-thaw cycles using a mixture of dry ice and ethanol and a water bath. Lysates were centrifuged at 16,000× *g* for 10 min at 4 °C, supernatant volumes were measured and exact volumes were transferred to fresh tubes and filled up to 19.6 µL with TSDG buffer. Each sample was incubated in a reaction volume of 20 µL after the addition of 0.5 µM Cy5-tagged pan-proteasomal activity-based probes (ABP) for one hour at 37 °C. Rat hybridoma assay controls were prepared as follows: 5 µg total protein extract was incubated (a) without proteasomal inhibitor and ABP, (b) 0.5 µM ABP, (c) 2 µM epoxomicin (Enzo, New York, NY1 h, 37 °C), followed by 0.5 µM ABP, (d) 2 µM ONX 0914 (1 h, 37 °C), followed by 0.5 µM ABP or (e) 0.1 µM ONX 0914 (1 h, 37 °C), and followed by 0.5 µM ABP. PTECs were incubated with 0.5 µM ABP. Thereafter, samples were mixed with a reducing sample buffer (50 mM Tris-HCl pH 6.8, 2% SDS, 100 mM DTT, 10% glycerol, 0.05% bromphenol blue) and boiled at 70 °C for 10 min. Samples were separated by SDS PAGE (12.5% self-cast gel from a 29:1 acrylamide/bis solution; Serva, Heidelberg, Germany) and imaged using a Vilber Fusion FX07 system (light capsule C640 and Filter F710) for measurement of proteasomal subunit activities. After that, samples were blotted on a PVDF membrane (Merck), and they were incubated with antibodies for the quantification of proteolytic proteasomal subunit protein abundance. The following antibodies were used: rabbit anti-β1c (PSMB6), rabbit anti-β5c (PSMB5, both Invitrogen), and rabbit anti-β5i (Lmp7; self-made, Elke Krüger, Biochemistry Greifswald, Germany). To assess total protein abundance, a mouse anti-β-actin (Sigma Aldrich) antibody was used. Binding of the ABP to active proteasomal subunits induced a MW shift of a few kDa in comparison to the inactive proteasomal subunit to which no ABP was bound.

2.16. Sequencing Data

The RNA-seq data set of renal epithelial cells and hepatic endothelial cells isolated from WT mice were available from the NCBI Gene Expression Omnibus (GEO) repository (GSE134663), and they were originally published by Krausgruber et al. [43]. We defined a gene set of 10 genes, all associated with antigen cross-presentation. The means of Log_2cpm (counts per million; n = 3), which represents the respective gene expression level within the gene set, were shown in heat maps.

2.17. Statistical Analysis

Data were analyzed using the GraphPad Prism software (GraphPad software, San Diego, CA, USA). Statistical comparison was carried out using a Mann–Whitney U test or a one-way ANOVA with post analysis by Tukey–Kramer test. Data were presented

as medians. A p value of less than 0.05 was considered statistically significant with the following ranges * $p< 0.05$, ** $p< 0.01$, *** $p< 0.001$, and **** $p< 0.0001$.

3. Results

3.1. PTECs Express Proteins Crucial for Antigen Cross-Presentation

There is an increasing body of evidence that non-hematopoietic, tissue-resident cell populations, such as endothelial and epithelial cells, are regulators of organ-specific immune responses [43]. To address a potential contribution of renal epithelial cells to the modulation of $CD8^+$ T-cell responses, we created a gene expression analysis of epithelial cell adhesion molecule $(EpCAM)^+$ epithelial cells isolated from the kidneys of C57BL/6 mice by using a previously published RNA-seq dataset [43]. For our analysis, we used the Log_2cpm, which represent the gene expression levels, from a gene set of 10 genes associated with antigen cross-presentation. We determined strong gene expression of the Sec61 translocon subunits (*Sec61a1*, *Sec61b*, *Sec61g*), the ATPase VCP (*Vcp*), and the aminopeptidase LNPEP (*Lnpep*) as well as substantial expression of the immunoproteasome subunit LMP7 (proteasome beta type (*Psmb*)*8*) and MR (*Mrc1*), whereas the TAP transporters (*Tap1*, *Tap2*) and the NADPH oxidase NOX2 (*Cybb*) were less expressed (Figure 1A). The same analysis was done with $CD31^+$ endothelial cells from the liver, from which it has been shown that particularly LSECs have a high capacity for antigen cross-presentation [20–24]. Here, we found stronger expression of *Psmb8*, *Mrc1*, and *Tap1*, while *Sec61a1* and *Sec61b* were less expressed (Figure 1B). Thus, both renal epithelial cells and hepatic endothelial cells express genes associated with antigen cross-presentation.

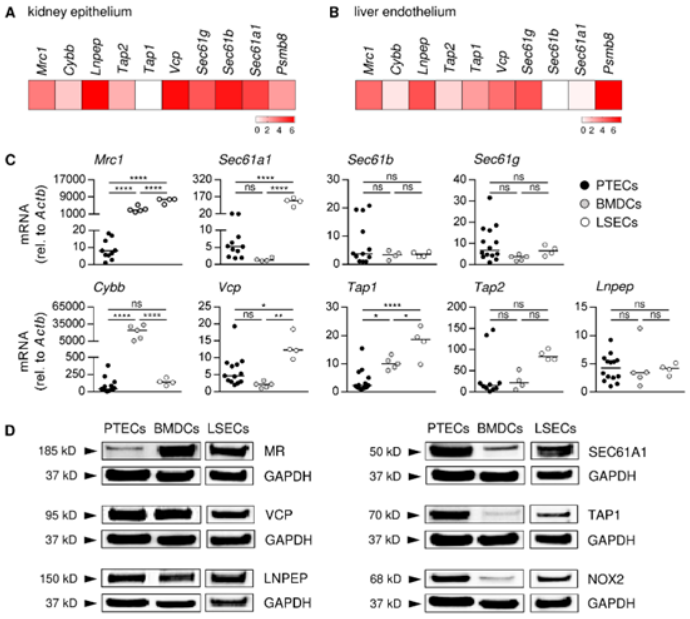

Figure 1. Gene and protein expression analysis of markers associated with antigen cross-presentation. RNA-seq data were used to create a gene set expression analysis of (**A**) renal epithelial cells and (**B**) liver endothelial cells. The Log_2cpm data sets were depicted in heat maps. (**C**) Gene expression profiles of PTECs, DCs, and LSECs were assessed by quantitative RT-PCR and normalized to the reference gene β-actin (*Actb*). Medians of at least four experiments are shown. (**D**) PTEC, DC, and LSEC protein expression levels were determined by a WB analysis and depicted in relation to expression of the reference protein GAPDH. Blots are representative of two experiments. * $p< 0.05$; ** $p< 0.01$; **** $p< 0.0001$; ns: not significant.

Within the different epithelial cell populations of the kidney, PTECs have been described as renal non-professional APCs that stimulate inflammatory $CD4^+$ T-cell activation [3,4]. Therefore, we asked whether PTECs are also able to activate $CD8^+$ T cells by antigen cross-presentation. We assessed expression of genes associated with cross-presentation in cultured PTECs and compared their expression profile with BMDCs, a population of professional APCs, and LSECs—a population of hepatic non-professional APCs—both capable of cross-presenting exogenous antigen to $CD8^+$ T cells [44,45]. Similar to the gene expression data of total renal epithelial cells, we found that PTECs expressed all genes that were included in our analysis. However, PTECs showed much less expression of *Mrc1* and *Tap1* in comparison to BMDCs and LSECs, whereas the gene expression levels of *Sec61b*, *Sec61g*, *Tap2*, and *Lnpep* were similar. PTECs and BMDCs showed a comparable expression of *Sec61a1* and *Vcp*, while the expression of both was increased in LSECs (Figure 1C). We then analyzed the expression of proteins involved in antigen cross-presentation in PTECs, comparing it to BMDCs and LSECs. We determined the expression of MR, TAP1, VCP, SEC61A1 (representative for the trimeric translocon), LNPEP, and NOX2 in PTECs. They showed a reduced MR expression compared to BMDCs and LSECs, while expression of TAP1 and NOX2 was elevated. The expression of SEC61A1 was enhanced in PTECs and LSECs compared to BMDCs, whereas VCP and LNPEP were expressed at the same level in all three cell populations (Figure 1D, Supplemental Figure S1). Thus, PTECs express genes and proteins associated with antigen cross-presentation.

3.2. PTECs Internalize Soluble Antigen via MR-Dependent Endocytosis

A prerequisite for antigen cross-presentation is internalization of exogenous antigen. To test the ability of PTECs for soluble antigen uptake, we incubated PTECs with the fluorochrome-labelled model antigen OVA at 37 °C or 4 °C at different periods of time. We determined an increased frequency of OVA^+ PTECs at 37 °C over time, which was strongly reduced after incubation at 4 °C (Figure 2A). The MR is an endocytic receptor, which has been implicated in soluble antigen uptake and cross-presentation [26,46]. To assess whether PTECs internalize OVA via the MR, they were pre-incubated with mannan, a polysaccharide that binds with a high affinity to the MR thereby competitively inhibiting MR-mediated endocytosis [41,47]. After the mannan treatment, the frequency of OVA^+ PTECs decreased compared to PTECs that were not pre-incubated with mannan. In contrast, pre-treatment of PTECs with D-galactose—a polysaccharide that does not bind to the MR [41]—did not affect uptake of OVA. Since internalization of the MR involves clathrin-coated vesicles, we analyzed the effect of the clathrin-specific inhibitor chlorpromazine (CPZ) [48] on antigen uptake through PTECs. We showed that the pre-incubation of PTECs with CPZ reduced their ability to take up OVA (Figure 2B). Thus, PTECs internalize soluble antigen via MR-mediated endocytosis.

3.3. PTECs Induce a Cytotoxic and Inflammatory Phenotype in $CD8^+$ T cells

We next analyzed the capacity of PTECs to induce an antigen-dependent activation of $CD8^+$ T cells via antigen cross-presentation. Therefore, we isolated OVA-specific $CD8^+$ $CD25^-$ T cells from the spleen and the lymph nodes of OT-I mice (Supplemental Figure S2), and we cultured them with PTECs in the presence or the absence of the antigen OVA for 2.5 days. As controls, $CD8^+$ $CD25^-$ T cells were cultured alone in the presence or the absence of OVA protein. To assess $CD8^+$ T-cell activation and proliferation, we stained for the activation markers CD25, CD44, and PD-1 as well as for the proliferation marker Ki-67. Without PTECs, $CD8^+$ T cells did not show any activation or proliferation. Moreover, PTECs did not induce substantial T-cell activation in absence of OVA. In contrast, we determined elevated frequencies of $CD8^+$ T cells expressing CD25, CD44, PD-1, and Ki-67 in the presence of PTECs and OVA (Figure 3A). We further analyzed the phenotype of PTEC-activated $CD8^+$ T cells, showing expression of the cytotoxic molecule granzyme B (GzmB). Since cytotoxic $CD8^+$ T cells store GzmB in granules, they must degranulate for its release to induce apoptosis in target cells. Expressed on membranes of such granules,

CD107a has been described as a degranulation marker, since it can only be detected on the cell surface after the fusion of granules with the cell membrane during degranulation [49,50]. We detected an elevated frequency of CD8$^+$ T cells expressing CD107a on the cell surface after activation through PTECs (Figure 3A), demonstrating their capacity for degranulation.

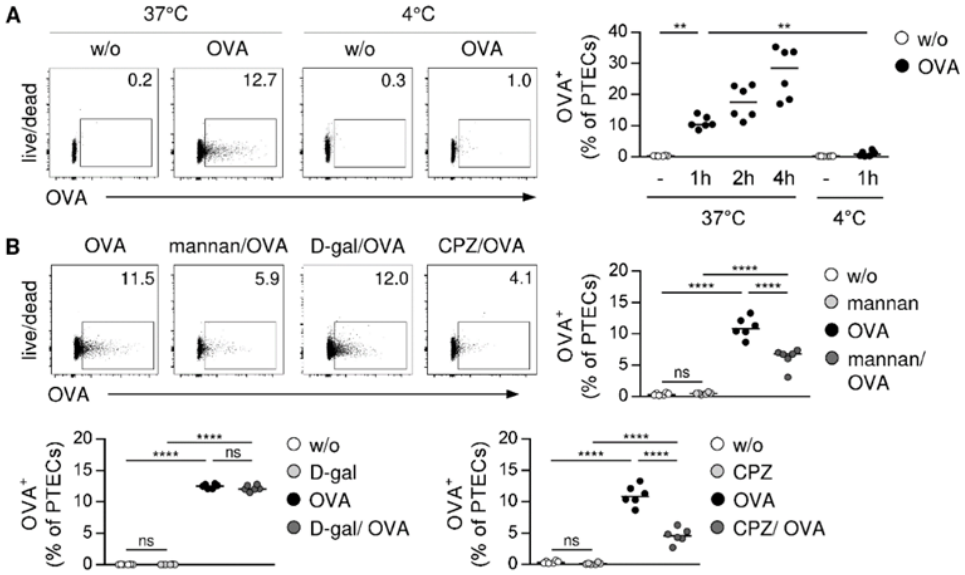

Figure 2. MR-mediated antigen uptake by PTECs. (**A**) PTECs were cultured in presence or absence of fluorochrome-labelled OVA at 37 °C or 4 °C over different periods of time and then analyzed by flow cytometry. (**B**) PTECs were pre-treated with mannan, D-galactose or CPZ before OVA incubation. Representative dot plots and medians of two experiments are shown. ** $p < 0.01$; **** $p < 0.0001$; ns: not significant; D-gal: D-galactose; CPZ: chlorpromazine; w/o: without.

By determining cytokine levels in culture supernatants, we found that CD8$^+$ T cells cultured alone did not express cytokines (data not shown). In contrast, we detected IL-2 and the inflammatory cytokines IFNγ, tumor necrosis factor (TNF)α, IL-17A, and IL-6 in co-culture supernatants of PTEC-activated CD8$^+$ T cells (Figure 3B), whereas anti-inflammatory cytokines such as IL-10 or type 2 cytokines such as IL-5 and IL-13 were not expressed (data not shown). We also performed a phenotype analysis of CD8$^+$ T cells after 5 days of culture. Again, CD8$^+$ T cells were not activated in the absence of PTECs. We showed that CD8$^+$ T cells were still activated, proliferated, and expressed CD107a and GzmB in the presence of PTECs and OVA (Supplemental Figure S3A). We further determined the same cytokine expression profile compared to CD8$^+$ T cells that were cultured for 2.5 days (Supplemental Figure S3B). Thus, PTECs induce an antigen-specific activation and proliferation of CD8$^+$ T cells, which express cytotoxic molecules and inflammatory cytokines.

3.4. PTECs Induce a Similar Phenotype in CD8$^+$ T Cells as Professional APCs

To assess the potential of PTECs for CD8$^+$ T-cell activation, we compared the phenotype of PTEC-activated CD8$^+$ T cells with CD8$^+$ T cells that were stimulated by professional DCs. Therefore, OVA-specific CD8$^+$ CD25$^-$ T cells were cultured with splenic DCs in the presence or the absence of OVA for 2.5 days. We performed viSNE analysis [51] to visualize the phenotype of CD8$^+$ T cells, which were either activated by PTECs or DCs. Clustering of CD8$^+$ T cells stained for activation and proliferation markers is depicted. We detected a similar clustering of PTEC- and DC-activated CD8$^+$ T cells with one cluster

characterized by a strong co-expression of CD44 and Ki-67, while the other cluster did not express Ki-67. The expression of CD25 co-localized with CD44 was much lower than CD44 expression; PD-1 expression was mainly determined in the Ki-67^{-} cluster (Figure 4A). In another viSNE analysis, we showed a comparable clustering of CD8^{+} T cells stained for markers associated with cytotoxicity. In both PTEC- and DC-activated CD8^{+} T cells, we found CD107a^{+} GzmB^{low} and CD107a^{low} GzmB^{+} clusters (Figure 4A), demonstrating the presence of degranulated and not degranulated CD8^{+} T cells, which differ in their amount of intracellularly stored GzmB.

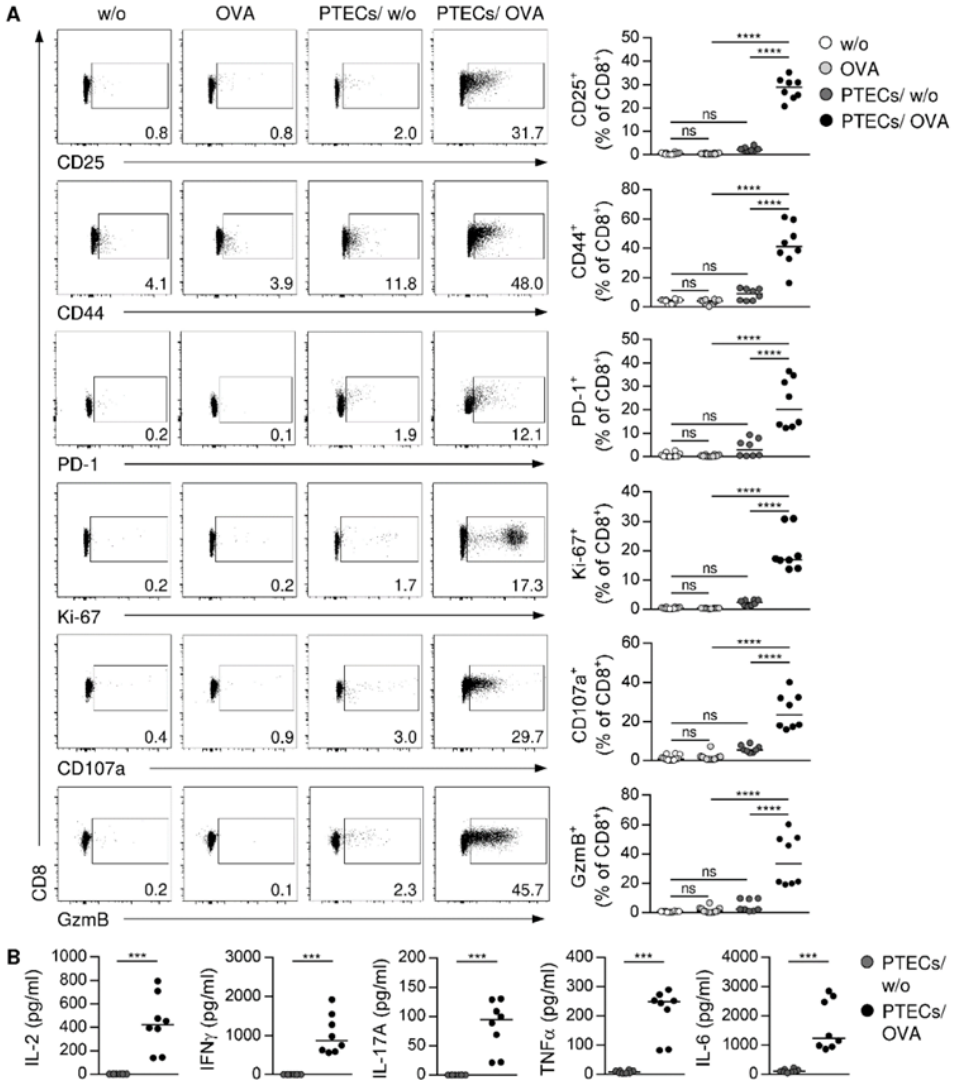

Figure 3. Antigen-dependent activation of CD8^{+} T cells by PTECs. OVA-specific CD8^{+} CD25^{-} T cells were cultured with PTECs or alone in presence or absence of OVA for 2.5 days. (**A**) CD8^{+} T cells were stained for CD25, CD44, PD-1, Ki-67, CD107a, and GzmB, and analyzed by flow cytometry. (**B**) Cytokine levels were determined in culture supernatants. Representative dot plots pre-gated on CD8^{+} TCRβ^{+} cells and medians of 2–3 experiments are shown. *** $p < 0.001$; **** $p < 0.0001$; ns: not significant; nd: not detectable; w/o: without OVA.

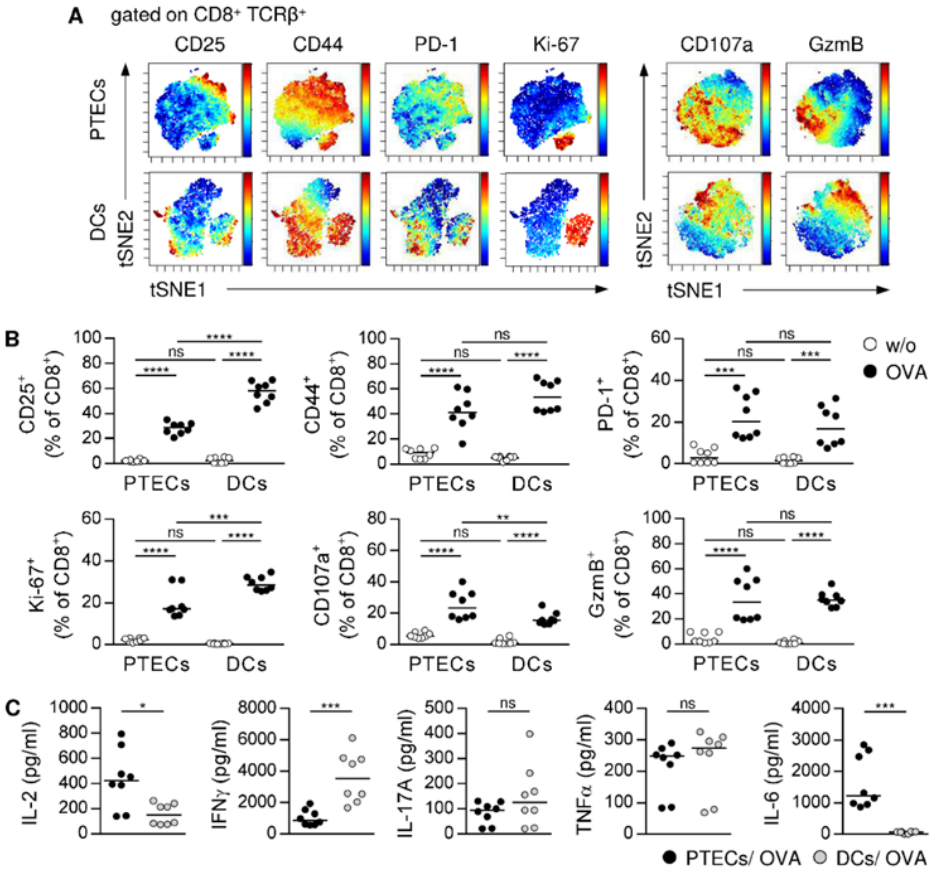

Figure 4. Phenotype analysis of CD8+ T cells activated by PTECs or splenic DCs. OVA-specific CD8+ CD25− T cells were cultured with PTECs or DCs in presence or absence of OVA for 2.5 days. (**A**) CD8+ T cells from co-cultures were stained for CD25, CD44, PD-1, and Ki-67 or CD107a and GzmB and analyzed by viSNE analysis. Single cells are represented by dots and expression levels are color coded from minimal (blue) to maximal (red). The viSNE analysis comprises 7955 PTEC-activated and 7829 DC-activated CD8+ T cells. (**B**) Phenotype of CD8+ T cells from co-cultures were analyzed by flow cytometry. (**C**) Cytokine levels were determined in co-culture supernatants. Representative tSNE plots and medians of two experiments are shown. * $p < 0.05$; ** $p < 0.01$; *** $p < 0.001$; **** $p < 0.0001$; ns: not significant; w/o: without OVA.

We showed a decreased frequency of PTEC-activated CD8+ T cells expressing CD25 and Ki-67 compared to CD8+ T cells activated by DCs. Both CD8+ T-cell populations showed the same expression of CD44, PD-1 and GzmB, whereas the expression of CD107a was elevated in PTEC-activated CD8+ T cells (Figure 4B). Additionally, DCs did not induce an expression of Th2 cytokines or IL-10 in CD8+ T cells (data not shown). However, DCs induced a stronger expression of IFNγ, while IL-17A and TNFα levels were comparable. Interestingly, we detected high levels of IL-6 in PTEC co-culture supernatants, whereas in DC co-cultures, IL-6 was not detectable (Figure 4C). After 5 days of co-culture, PTEC-activated CD8+ T cells still proliferated less and showed a reduced expression of PD-1, CD107a, and IFNγ than CD8+ T cells activated by DCs, while expression of GzmB was comparable (Supplemental Figure S4A,B). In contrast, IL-2 and TNFα level were increased in PTEC/CD8 co-culture supernatants (Supplemental Figure S4B). Thus, PTEC-stimulated

CD8$^+$ T cells are less activated than DC-stimulated CD8$^+$ T cells, but they show a similar cytotoxic and inflammatory phenotype.

3.5. Different Outcome of CD8$^+$ T-Cell Activation Induced by Non-Professional APCs from Kidney and Liver

To assess the organ-specific characteristics of non-professional APC-mediated CD8$^+$ T-cell activation, we did a comparative phenotype analysis of CD8$^+$ T cells that were either activated by PTECs or LSECs. Therefore, OVA-specific CD8$^+$ CD25$^-$ T cells were cultured with LSECs in the presence or the absence of OVA for 2.5 days. Compared to PTECs, LSECs induced the same level of activation, proliferation, and expression of cytotoxic molecules and inflammatory cytokines in CD8$^+$ T cells. In contrast, IL-2 levels were decreased in LSEC co-cultures (Supplemental Figure S5A,B). Interestingly, we found a striking difference in the phenotype of activated CD8$^+$ T cells after 5 days of co-culture. While CD8$^+$ T cells activated by PTECs still proliferated and expressed cytotoxic molecules and inflammatory cytokines, LSEC-stimulated CD8$^+$ T cells were still activated but no longer proliferated or expressed GzmB and CD107a (Figure 5A). They further showed a strongly reduced expression of IFNγ in comparison to PTEC-activated CD8$^+$ T cells. Moreover, we did not detect IL-2 in LSEC co-culture supernatants (Figure 5B), most likely through consumption of the little IL-2 that was produced in the beginning by CD8$^+$ T cells. Thus, in contrast to LSECs, PTECs do not have the ability to inhibit initial inflammatory CD8$^+$ T-cell activation.

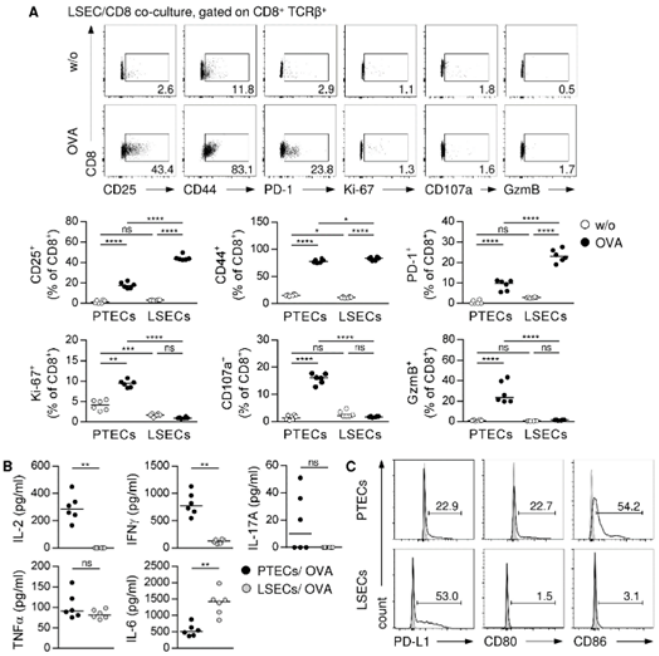

Figure 5. Phenotype analysis of CD8$^+$ T cells activated by PTECs or LSECs. OVA-specific CD8$^+$ CD25$^-$ T cells were cultured with PTECs or LSECs in presence or absence of OVA for 5 days. (**A**) CD8$^+$ T cells from co-cultures were stained for CD25, CD44, PD-1, Ki-67, GzmB, and CD107a and analyzed by flow cytometry. (**B**) Cytokine levels were determined in co-culture supernatants. Representative dot plots of LSEC/CD8 co-cultures and medians of two experiments are shown. (**C**) PTECs and LSECs were stained for PD-L1, CD80, and CD86 and analyzed by flow cytometry. Representative dot plots of two experiments are shown. * $p < 0.05$; ** $p < 0.01$; *** $p < 0.001$; **** $p < 0.0001$; ns: not significant; w/o: without OVA.

LSECs have been shown to induce inhibition of effector CD8$^+$ T cells by the programmed cell death (PD)-1/PD-L1 pathway [52,53]. While expression of the co-inhibitory receptor PD-1 was comparable in PTEC- and LSEC-activated CD8$^+$ T cells after short culture time (Supplemental Figure S5A), we determined an elevated expression of PD-1 by LSEC-stimulated CD8$^+$ T cells after 5 days of co-culture (Figure 5A). Moreover, the frequency of LSECs expressing the co-inhibitory ligand PD-L1 increased compared to PTECs, whereas expression of the co-stimulatory molecules CD80 and CD86 was mainly observed in PTECs (Figure 5C). Thus, PTECs and LSECs differ in their expression of co-inhibitory and co-stimulatory molecules.

3.6. PTEC-Induced CD8$^+$ T-Cell Activation Depends on Proteasome Activity

The immunoproteasome plays a crucial role in antigen processing and subsequent T-cell activation; and, thus has become a target in autoimmune diseases [54]. To assess a potential contribution of the immunoproteasome in antigen cross-presentation by PTECs, we analyzed gene and protein expression of LMP7, a catalytic subunit selectively present in the immunoproteasome. We showed gene expression of *Psmb8* and protein expression of LMP7 by PTECs (Figure 6A,B). In comparison to BMDCs and LSECs, PTECs expressed much less LMP7 (Figure 6B). The pre-treatment of PTECs with the LMP7 inhibitor ONX 0914 [54] impaired PTEC-induced CD8$^+$ T-cell activation. We determined a reduced frequency of activated and proliferating CD8$^+$ T cells, and the expression of GzmB was also strongly decreased. The analysis was done after 1.5 days of co-culture, and at this time point the degranulation capacity of PTEC-activated CD8$^+$ T cells was still minor as demonstrated by the low frequency of CD107a$^+$ CD8$^+$ T cells, which was further reduced after pre-treatment of PTECs with ONX 0914 (Figure 6C). Moreover, cytokine levels in co-culture supernatants were strongly diminished (Figure 6D), further demonstrating the impaired capacity of PTECs to induce inflammatory CD8$^+$ T-cell activation after pre-incubation with ONX 0914.

To address the specificity of ONX 0914-induced proteasome inhibition in PTECs, proteolytic activities and the protein expression of subunits present in the immunoproteasome or the constitutive proteasome were analyzed. In western blot (WB) analysis, we showed a higher abundance of the immunoproteasome-specific subunit β5i (LMP7) in ONX 0914-treated PTECs compared to untreated PTECs. However, protein abundance of β5c and β1c was also enhanced, which are two subunits of the constitutive proteasome (Figure 6E, Supplemental Figure S6A). We further determined a complete binding of both β5i and β5c by ONX 0914 (Figure 6E). We used ABPs that react with proteasomes in relation to their catalytic activity to assess proteolytic activity of the different proteasome subunits. The treatment of PTECs with ONX 0914 resulted in the strongly reduced activity of β5i and β5c, whereas β1c and β2c activity was not substantially altered (Figure 6E, Supplemental Figure S6B). Thus, by binding to β5i and β5c, ONX 0914 not only inhibited the proteolytic activity of an immunoproteasome subunit but also of a subunit present in the constitutive proteasome in PTECs.

3.7. PTEC-Activated CD8$^+$ T Cells Exert Cytotoxic Function

PTEC-activated CD8$^+$ T cells express the cytotoxic molecule GzmB and the degranulation marker CD107a, indicating that PTECs induce cytotoxicity in CD8$^+$ T cells. To analyze the cytotoxic function of PTEC-activated CD8$^+$ T cells, we performed a cytotoxicity assay with allogenic P815 target cells [42]. In this assay, cytotoxic CD8$^+$ T cells become activated through interaction of their TCR with allogenic MHC molecules on P815 cells, resulting in induction of cell death in the target cells. Therefore, PTEC-activated CD8$^+$ T cells were cultured with P815 cells for four hours. Subsequently, target cell killing was assessed by 7-AAD staining. As controls, P815 cells were incubated with CD8$^+$ T cells pre-cultured with or without PTECs in the presence or the absence of OVA. Thereafter, the frequency of 7-AAD$^+$ P815 cells was analyzed. Compared to P815 cells cultured alone, we determined no increased P815 cell death in the presence of CD8$^+$ T cells pre-cultured without PTECs. The frequency of 7-AAD$^+$ P815 cells increased if CD8$^+$ T cells from PTECs pre-cultures

without OVA were used. Interestingly, we determined a strongly elevated frequency of the 7-AAD$^+$ P815 cell in the presence of CD8$^+$ T cells that were pre-cultured with PTECs and OVA (Figure 7), demonstrating the cytotoxic function of PTEC-activated CD8$^+$ T cells.

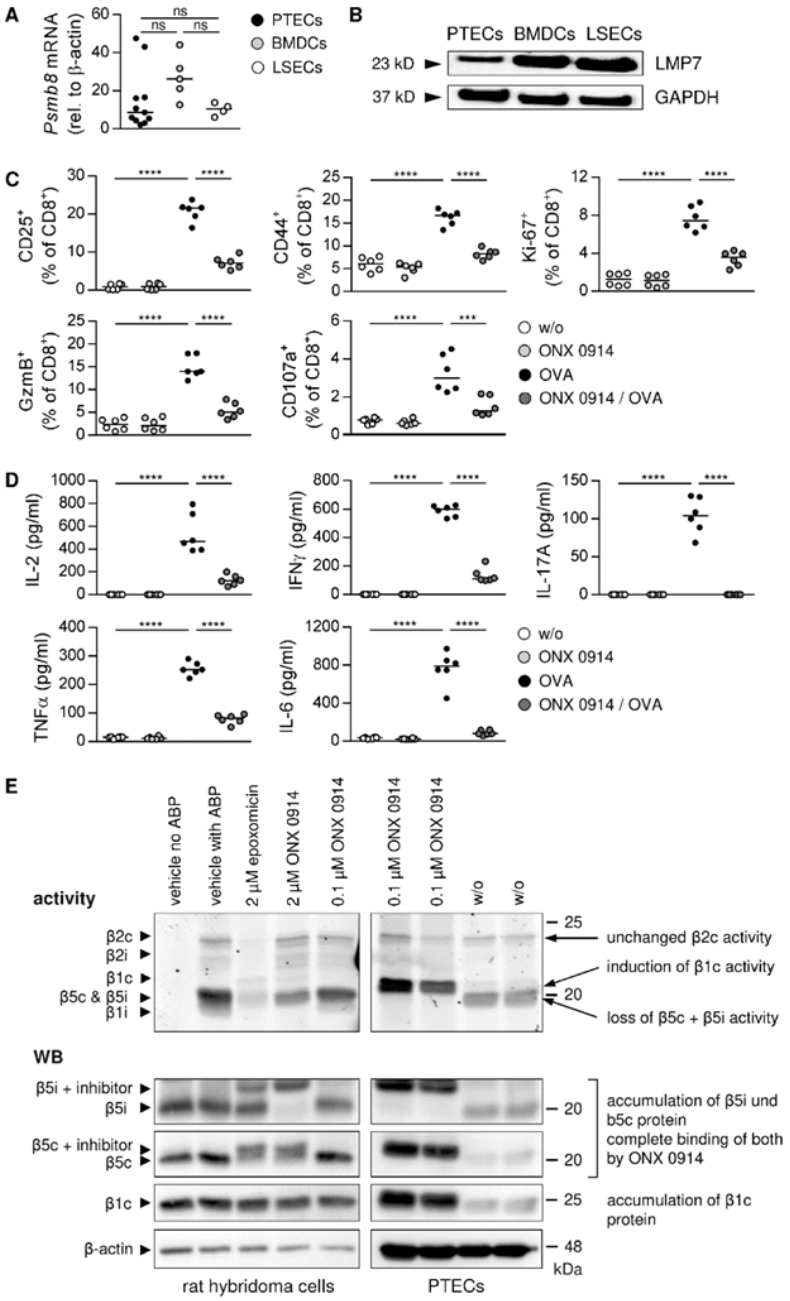

Figure 6. Proteasome-dependent CD8$^+$ T-cell activation. (**A**) Expression of *Psmb8* was analyzed in PTECs, BMDCs, and LSECs by quantitative RT-PCR and normalized to the reference gene β-actin.

Medians of at least four experiments are shown. (**B**) LMP7 protein expression was determined by WB analysis and depicted in relation to expression of the reference protein GAPDH. Blots are representative of two experiments. (**C**) PTECs were pre-incubated with ONX 0914 before co-culture with $CD8^+$ T cells in presence and absence of OVA for 1.5 days. Phenotype of $CD8^+$ T cells was analyzed by flow cytometry. (**D**) Cytokine levels were determined in culture supernatants. (**E**) PTECs were incubated with ONX 0914. Rat hybridoma cells were incubated with the proteasome inhibitor epoxomicin or ONX 0914. Activities of catalytic proteasome subunits were assessed by using ABPs. Protein expression of the different catalytic subunits was determined by WB analysis. Blots are representative of two experiments. Medians of two experiments are shown. *** $p < 0.001$; **** $p < 0.0001$; ns: not significant; w/o: without.

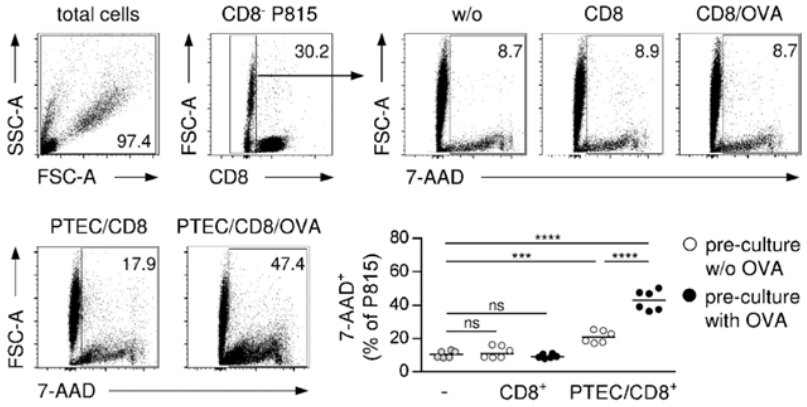

Figure 7. Cytotoxic function of PTEC-activated $CD8^+$ T cells. $CD8^+$ T cells pre-cultured with and without PTECs in presence or absence of OVA were incubated with allogenic P815 target cells for four hours. Cells were stained for 7-AAD and CD8 and analyzed by flow cytometry. Representative dot plots and medians of two experiments are shown. *** $p < 0.001$; **** $p < 0.0001$; ns: not significant; w/o: without; PTEC/CD8: $CD8^+$ T cells pre-cultured with PTECs; CD8: $CD8^+$ T cells pre-cultured alone.

3.8. $CD8^+$ T Cell-Dependent Induction of Apoptotic Cells Death in Murine Lupus Nephritis

Activation of $CD8^+$ T cells by PTECs requires cell contact in the kidney. To assess localization of $CD8^+$ T cells in murine immune-mediated GN, we stained for CD8 and the T-cell marker CD3 in serial kidney sections of healthy and diseased mice. The MRL-*lpr* mice were used as a model of systemic lupus erythematosus (SLE) to study localization of $CD8^+$ T cells in lupus nephritis. At an age of 15 weeks, MRL-*lpr* mice showed elevated plasma autoantibody levels, an increased renal activity score [37], and proteinuria compared to MRL mice (Supplemental Figure S7A). In the naïve kidney, the number of $CD8^+$ T cells was very low. We determined an elevated $CD8^+$ T-cell number in the inflamed kidney, which predominantly localized in the tubulointerstitium. The number of $CD8^+$ T cells within glomeruli was also increased although in lower numbers than in the tubulointerstitium of MRL-*lpr* mice (Figure 8A). We further assessed renal $CD8^+$ T-cell localization in pristane-induced lupus nephritis. Here, pristane-treated WT mice developed autoantibodies and glomerular injury within nine months (Supplemental Figure S7B). Again, the majority of $CD8^+$ T cells was localized in the tubulointerstitium of pristane-treated mice, and we detected only a low number within glomeruli (Figure 8B). Thus, in lupus nephritis, $CD8^+$ T cells mainly accumulate in the tubulointerstitium, which enables close contact to PTECs.

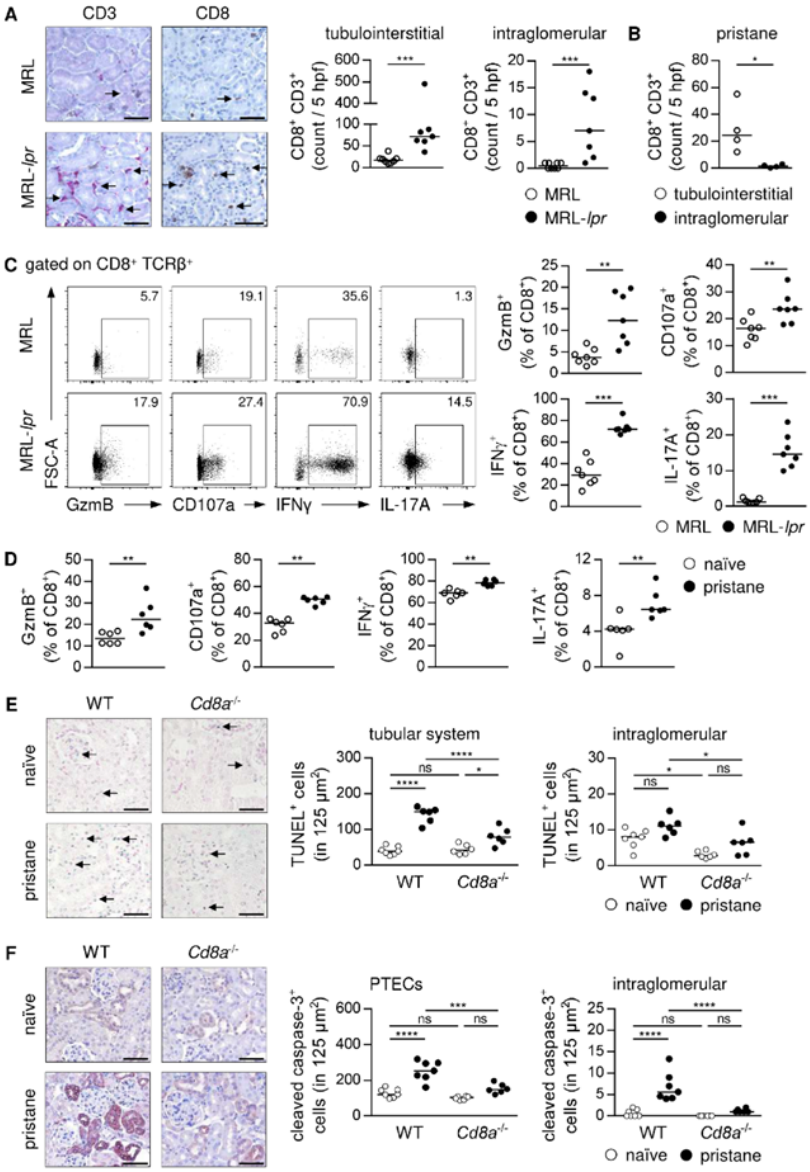

Figure 8. CD8$^+$ T cell-dependent apoptosis in murine lupus nephritis. Serial kidney sections of (**A**) lupus-prone MRL-*lpr* mice and (**B**) pristane-treated WT mice were stained with anti-CD3 or anti-CD8 antibodies. Number of tubulointerstitial and intraglomerular CD8$^+$ CD3$^+$ T cells were counted in 5 hpf per section. Arrows mark CD8$^+$ T cells. (**C**) Phenotype of renal CD8$^+$ T cells was analyzed in MRL-*lpr* mice and (**D**) pristane-treated WT mice by flow cytometry. (**E**) Number and localization of renal apoptotic cells and (**F**) cleaved caspase-3$^+$ cells were analyzed by TUNEL assay or cleaved caspase-3 staining in pristane-treated WT and *Cd8a*$^{-/-}$ mice. Bars represent 50 µm. Representative dot plots and medians of one out of two experiments are shown. * $p < 0.05$; ** $p < 0.01$; *** $p < 0.001$; **** $p < 0.0001$, ns: not significant.

We then analyzed the phenotype of renal CD8$^+$ T cells in murine lupus nephritis. We detected elevated frequencies of CD8$^+$ T cells expressing GzmB, CD107a, IFNγ, and IL-17A in MRL-*lpr* mice compared to MRL mice (Figure 8C). The same phenotype was observed in pristane-treated WT mice compared to age-matched naïve WT mice (Figure 8D), demonstrating a cytotoxic and an inflammatory phenotype of CD8$^+$ T cells that infiltrate the kidney in lupus nephritis. As cytotoxic CD8$^+$ T cells induce apoptosis in target cells, we performed a TUNEL staining to detect apoptotic cells in renal tissue. We determined an increased number of TUNEL$^+$ cells in pristane-treated WT mice compared to healthy controls, which were mainly localized in the tubular system. Interestingly, lack of CD8$^+$ T cells in *Cd8a*$^{-/-}$ mice resulted in a reduced number of TUNEL$^+$ tubular cells in lupus nephritis (Figure 8E). One mechanism by which GzmB induces apoptotic cell death is via activation of caspase-3 through proteolytic processing [55]. Therefore, we stained for cleaved caspase-3, the active form of this enzyme, in renal tissue. We found highly up-regulated expression of cleaved caspase-3 in pristane-treated WT mice compared to naïve mice. Particularly proximal tubuli showed expression of cleaved caspase-3, but we also detected an increased number of cleaved caspase-3$^+$ cells within glomeruli. Induction of renal cleaved caspase-3 expression was strongly reduced in pristane-treated *Cd8a*$^{-/-}$ mice in comparison to diseased WT mice (Figure 8F), further demonstrating the importance of CD8$^+$ T cells for induction of apoptotic cell death in lupus nephritis. As MRL-*lpr* mice bear a mutation in the gene encoding Fas and are therefore not able to induce apoptotic cell death via the Fas/FasL pathway, which also targets caspase-3, the number of TUNEL$^+$ cells and cleaved caspase-3$^+$ cells were reduced in the kidneys of MRL-*lpr* mice compared to MRL mice (Supplemental Figure S7C,D), suggesting that apart from GzmB-induced cell death the Fas/FasL pathway also contributes to induction of apoptosis in lupus nephritis.

4. Discussion

Immune-mediated GN comprises a group of life-threatening diseases triggered by so far poorly defined mechanisms. Thus, identifying immunological pathways involved in disease pathology is of high clinical relevance. The outcome of an immune response depends on different factors such as the type of APC population, which initiates T-cell activation. While professional DCs promote CD8$^+$ T cell-mediated immunity [12,15,16], non-professional LSECs favor induction of tolerance [22–24]. In this study, we described PTECs as a population of renal non-professional APCs that facilitate immunity by inducing cytotoxic and inflammatory CD8$^+$ T cells via cross-presentation of soluble antigen in vitro.

By performing expression analyses, we showed that PTECs expressed genes and proteins involved in receptor-mediated internalization of soluble antigen into endosomes, antigen translocation into cytosol, proteasomal antigen degradation, transport of antigen-derived peptides back into endosomes, peptide trimming and endosomal alkalization, altogether indicating that PTECs have the capacity for antigen cross-presentation via the endosome-to-cytosol pathway [25]. A comparison between mRNA and protein data revealed that mRNA abundances determined in the different cell populations only partially reflected the respective protein abundances. This is in line with studies demonstrating that mRNA levels can only explain to some extent variations in protein levels, which are differentially regulated in certain cell types. Ratios between mRNA and protein are mainly determined by protein translation and degradation. Protein levels also depend on protein function since less stable proteins allow rapid alterations in gene and subsequent protein responses to certain stimuli, e.g., inflammation [56,57]. Since we compared three different cell populations from which only BMDCs are classical APCs, while PTECs and LSECs also fulfil other organ-specific physiological functions, translation and degradation of the analyzed proteins may be differentially regulated in the cell populations leading to discrepancies in mRNA and protein abundances.

Although PTECs expressed less MR than BMDCs and LSECs, we provided evidence that PTECs can use the MR for antigen uptake. By using fluorochrome-labelled OVA, we showed that PTECs internalized soluble antigen at 37 °C. Since OVA internalization was

abrogated at 4 °C, this demonstrates an energy-dependent process and excludes unspecific binding of OVA on the cell surface. The MR has been implicated in soluble, mannosylated antigen internalization thereby promoting transport into endosomes for antigen cross-presentation [26,46]. We demonstrated that PTECs internalized soluble antigen via the MR—as blockage of the receptor by mannan decreased OVA uptake—whereas another sugar, which does not bind to the MR, did not affect antigen uptake. MR internalization occurs in clathrin-coated vesicles at the plasma membrane before transport to cytosolic endosomes. We showed that by preventing formation of clathrin-coated vesicles through CPZ [48], OVA uptake in PTECs was diminished. Based on these findings, we conclude that PTECs can internalize soluble antigen via MR-mediated endocytosis. Thus, PTECs exploit a well-described pathway of antigen uptake as DCs [47,58] and LSECs [59] have also been shown to internalize soluble antigen via the MR.

In the co-culture experiments using OVA protein as a soluble antigen, we showed an antigen-dependent activation and proliferation of $CD8^+$ T cells in the presence of PTECs. Since in the controls without OVA or PTECs $CD8^+$ T cells were not activated, this demonstrates the ability of PTECs to present a soluble antigen to $CD8^+$ T cells thereby stimulating their activation. As a prerequisite, proteasomal degradation of internalized protein into antigenic peptides must be performed. We found that PTECs expressed the immunoproteasome-specific catalytic subunit LMP7, although its expression was diminished compared to BMDCs and LSECs. Pre-incubation of PTECs with the LMP7 inhibitor ONX 0914 resulted in a reduced activation and proliferation of $CD8^+$ T cells. We showed that PTECs favor induction of immunity as PTEC-activated $CD8^+$ T-cell expressed inflammatory cytokines, expressed the cytotoxic molecule GzmB and exerted a cytotoxic function by killing allogenic target cells. Both the expression of GzmB and the inflammatory cytokines were decreased after pre-treatment of PTECs with ONX 0914, suggesting that the immunoproteasome is involved in PTEC-mediated inflammatory $CD8^+$ T-cell activation. However, our data showed that ONX 0914 not only bound to LMP7 but also to β5c thereby inhibiting the proteolytic activities of subunits that are present in the immunoproteasome or in the constitutive proteasome. This also explains the observed elevated protein abundance in ONX 0914-treated PTECs since inhibition of a catalytic subunit of the constitutive proteasome impairs regular protein degradation, leading to intracellular protein accumulation. Treatment of ONX 0914 further resulted in highly up-regulated expression of β1c in PTECs, without affecting its proteolytic activity. Since we also did not detect altered activity of β2c, another catalytic subunit of the constitutive proteasome, we conclude that PTECs can use LMP7 and β5c to generate antigenic peptides for cross-presentation to induce cytotoxic and inflammatory $CD8^+$ T cells.

As shown for LSECs in the liver [22–24], non-professional APCs can induce another phenotype in activated $CD8^+$ T cells than professional APCs, which influences the outcome of an immune response. We therefore compared the phenotype of PTEC-activated $CD8^+$ T cells with those stimulated by splenic DCs or LSECs. After 2.5 days of co-culture, we found that all three APC populations induced expression of GzmB and inflammatory cytokines in $CD8^+$ T cells. PTEC-induced $CD8^+$ T-cell activation, proliferation, and IFNγ expression was reduced compared to DCs, illustrating the different capacities of professional and non-professional APCs for T-cell activation. In contrast, PTECs and LSECs did not differ in their potential to activate $CD8^+$ T cells at this time point of analysis, but we determined a strongly reduced expression of IL-2 in LSEC-activated $CD8^+$ T cells. Interestingly, there was a striking difference in the phenotype of activated $CD8^+$ T cells after 5 days of co-culture. While PTEC- and DC-activated $CD8^+$ T cells showed a sustained proliferation and expression of cytotoxic molecules and inflammatory cytokines, this was not the case for LSEC-stimulated $CD8^+$ T cells. Here, $CD8^+$ T cells no longer proliferated or expressed GzmB, and they also lost the capacity for degranulation, a prerequisite for the cytotoxic function. Moreover, they lacked expression of IL-2, and they showed strongly reduced production of IFNγ. These data are in line with previous studies, demonstrating functional inactivation of $CD8^+$ T cells by LSECs [52,53,60,61]. Mechanistically, LSECs were

shown to up-regulate expression of PD-L1 during co-culture with $CD8^+$ T cells, thereby inducing a co-inhibitory signal in initially activated $PD\text{-}1^+$ $CD8^+$ T cells [52,53]. A low expression of co-stimulatory molecules and an impaired capacity to induce IL-2 expression in activated $CD8^+$ T cells have also been identified as mechanisms of LSEC-induced $CD8^+$ T-cell tolerance [53,60,61]. By comparing the expression of co-inhibitory and co-stimulatory molecules, we found that PTECs expressed less PD-L1 but much more CD80 and CD86 than LSECs, and in contrast to LSECs, they induced a strong and a sustained IL-2 expression in $CD8^+$ T cells. These differences between PTECs and LSECs provide an explanation for the different outcome of $CD8^+$ T-cell activation induced by non-professional APCs from the kidney and the liver. While LSECs limit $CD8^+$ T-cell responses, thereby inducing tolerance against oral and tumor-derived antigens [22–24], PTECs support the induction of cytotoxic and inflammatory $CD8^+$ T cells, which may contribute to the pathogenesis of immune-mediated GN.

In human lupus nephritis, $CD8^+$ T cells have been shown to infiltrate the kidney [62,63], where accumulation of periglomerular $CD8^+$ T cells correlated with disease severity [64], suggesting that they may contribute to disease pathology. In addition, renal $CD8^+$ T cells expressing GzmB or another granzyme, GzmK, have been identified in lupus nephritis patients [65]. A pathogenic role of $CD8^+$ T cells has also been described in different mouse models of immune-mediated GN [66]. However, how $CD8^+$ T cells become activated in GN and the mechanisms by which they contribute to disease pathology is less clear. In murine lupus nephritis, the majority of kidney-infiltrating $CD8^+$ T cells accumulated in the tubulointerstitium in close contact to proximal tubuli. Based on the in vitro studies, it may be conceivable that PTECs cross-present antigens in immune-mediated GN thereby promoting cytotoxic $CD8^+$ T cells, which may induce apoptotic cell death in the tubular system, e.g., by release of GzmB, which thereby promotes tubulointerstitial nephritis. Our assumption that $CD8^+$ T cells exert a cytotoxic function in immune-mediated GN is supported by the finding that the observed apoptotic cell death in the tubular system of mice with lupus nephritis was reduced in the absence of $CD8^+$ T cells. Moreover, particularly PTECs showed an elevated expression of the active form of caspase-3 in lupus nephritis—an enzyme involved in the induction of apoptotic cell death—whose proteolytic activation can be induced by GzmB [55]. Interestingly, a lack of $CD8^+$ T cells impaired activation of caspase-3 in PTECs, further indicating the key role of $CD8^+$ T cells in the induction of apoptosis in murine lupus nephritis, which may mainly affect cross-presenting PTECs.

We also detected $CD8^+$ T cells within glomeruli in lupus nephritis raising the question of whether they may contribute to glomerular damage in immune-mediated GN. Crescent formation is a hallmark of severe glomerular injury involving proliferation of cells in Bowman's space as a result of damage in the capillary wall, glomerular basement membrane, and Bowman´s capsule, which lead to fibrin formation and induction of inflammatory immune responses [67]. The role of $CD8^+$ T cells in these pathogenic processes is less clear. Two studies indicated that antigen-specific $CD8^+$ T cells can infiltrate the glomeruli during autoimmune GN, if the Bowman´s capsule is destroyed, and kill intraglomerular cells such as podocytes, which present autoantigens [68,69]. Thus, cytotoxic $CD8^+$ T cells may be responsible for the progression of glomerular damage in severe immune-mediated GN by killing antigen-presenting cells within glomeruli. Indeed, it has been shown that podocytes can function as renal APCs [70].

Cross-presentation of self-antigens has been implicated in the development of autoimmune diseases [18]. In one study, albumin was suggested as a self-antigen in renal disease with proteinuria, where breakdown of the glomerular filtration barrier results in access of albumin to kidney tissue. The authors demonstrated the generation of albumin-derived antigenic peptides through a concerted action of PTECs and DCs in vitro, resulting in DC-induced inflammatory $CD8^+$ T-cell activation [71]. Whether PTECs are also capable of cross-presenting albumin-derived peptides has not been analyzed so far, but it may be possible that PTECs could thereby contribute to the development of autoimmune kidney disease.

In summary, this study revealed the capacity of PTECs for antigen cross-presentation thereby inducing cytotoxic and inflammatory $CD8^+$ T cells, and it further identified $CD8^+$ T cells to induce apoptosis in the tubular system in murine lupus nephritis. The predominant in vitro data open the possibility for hypotheses about the in vivo relevance of PTEC-mediated $CD8^+$ T-cell activation for disease pathology of immune-mediated GN. However, it remains an important open question whether PTECs cross-present self-antigens in autoimmune kidney disease thereby becoming a target for cytotoxic $CD8^+$ T cells.

Supplementary Materials: The following supporting information can be downloaded at: https://www.mdpi.com/article/10.3390/cells11091510/s1, Figure S1: Quantitative WB analysis.; Figure S2: Purity of isolated $CD8^+$ T cells.; Figure S3: Antigen-dependent activation of $CD8^+$ T cells by PTECs after 5 days of co-culture.; Figure S4: Phenotype analysis of $CD8^+$ T cells activated by PTECs or DCs after 5 days of co-culture.; Figure S5: Phenotype analysis of $CD8^+$ T cells activated by PTECs or LSECs after 2.5 days of co-culture.; Figure S6: Protein expression and catalytic activities of proteasome subunits.; Figure S7: Renal pathology in murine lupus nephritis models.; Table S1: Sequences of the primer used for analysis of mRNA expression.

Author Contributions: A.L.: performed experiments, analyzed and interpreted data, and revised manuscript; H.C.: performed experiments and analyzed and interpreted data; A.M.: performed experiments, analyzed data, and revised manuscript; C.M.-S.: analyzed and interpreted data; S.M.: analyzed data and revised manuscript; T.W.: analyzed data and revised manuscript; C.W.: performed experiments, analyzed data and revised manuscript; J.R.: performed experiments and analyzed data; O.M.S.: design of research and revised manuscript; L.D.: design of research and revised manuscript; G.T.: conception and design of research and revised manuscript; K.N.: conception and design of research, performed experiments, analyzed and interpreted data and wrote the manuscript. All authors have read and agreed to the published version of the manuscript.

Funding: This work was supported by the Deutsche Forschungsgemeinschaft (DFG): SFB 1192 project B3 granted to C.M.-W., A3 granted to O.M.S, B6 granted to T.W. and A2 granted to G.T. and K.N.

Institutional Review Board Statement: The animal study protocol was approved by the Institutional Review Board (or Ethics Committee) of the Behörde für Justiz und Verbraucherschutz (Hamburg, Germany; approval codes: N57/19 (09.2019), ORG 960 (04.2019), ORG 1032(10.2020)).

Informed Consent Statement: Not applicable.

Data Availability Statement: All data generated or analyzed during this study are included in this published article and its Supplementary Information.

Acknowledgments: The authors acknowledge the excellent technical assistance of Elena Tasika, Carsten Rothkegel (Institute of Experimental Immunology and Hepatology, University Medical Center Hamburg-Eppendorf, Hamburg, Germany) and Johannes Brand (Institute of Cellular and Integrative Physiology, University Medical Center Hamburg-Eppendorf, Hamburg, Germany). We also thank all members of the FACS Sorting Core Unit (University Medical Center Hamburg-Eppendorf, Hamburg, Germany) for cell sorting.

Conflicts of Interest: The authors declare no conflict of interest.

Abbreviations

7-AAD: 7-amino-actinomycin D, ABP: activity-based probe, ANCA: anti-neutrophil cytoplasmic autoantibody, APC: antigen-presenting cell, BMDCs: bone marrow-derived dendritic cells, CPZ: chlorpromazine, DC: dendritic cell, FACS: fluorescence-activated cell sorting, GN: glomerulonephritis, GzmB: granzyme B, hpf: high power field, HRP: horseradish peroxidase, LMP7: large multifunctional peptidase 7, LNPEP: leucyl-cystinyl aminopeptidase, LSEC: liver sinusoidal endothelial cell, IFN: interferon, IL: interleukin, MACS: magnetic-activated cell sorting, MHC-II: major histocompatibility complex class II, MR: mannose receptor, MRL: MRL/MpJ, MRL-*lpr*: MRL/MpJ-*Fas*^{lpr}/J, NOX2: NADPH oxidase 2, OVA: ovalbumin, PAS: periodic acid-Schiff, Psmb8: proteasome beta type 8, PTEC: proximal tubular epithelial cell, TAP1: transporter associated with antigen processing 1, TCR: T-cell receptor, TNF: tumour necrosis factor, VCP: valosin-containing protein, WB: western blot, WT: wild type.

References

1. Anders, H.-J.; Vielhauer, V.; Schlöndorff, D. Chemokines and Chemokine Receptors Are Involved in the Resolution or Progression of Renal Disease. *Kidney Int.* **2003**, *63*, 401–415. [CrossRef] [PubMed]
2. Lai, K.N.; Leung, J.C.K.; Chan, L.Y.Y.; Guo, H.; Tang, S.C.W. Interaction between Proximal Tubular Epithelial Cells and Infiltrating Monocytes/T Cells in the Proteinuric State. *Kidney Int.* **2007**, *71*, 526–538. [CrossRef] [PubMed]
3. Hagerty, D.T.; Allen, P.M. Processing and Presentation of Self and Foreign Antigens by the Renal Proximal Tubule. *J. Immunol.* **1992**, *148*, 2324–2330.
4. Breda, P.C.; Wiech, T.; Meyer-Schwesinger, C.; Grahammer, F.; Huber, T.; Panzer, U.; Tiegs, G.; Neumann, K. Renal Proximal Tubular Epithelial Cells Exert Immunomodulatory Function by Driving Inflammatory CD4+ T Cell Responses. *Am. J. Physiol. Ren. Physiol.* **2019**, *317*, F77–F89. [CrossRef] [PubMed]
5. Gastl, G.; Ebert, T.; Finstad, C.L.; Sheinfeld, J.; Gomahr, A.; Aulitzky, W.; Bander, N.H. Major Histocompatibility Complex Class I and Class II Expression in Renal Cell Carcinoma and Modulation by Interferon Gamma. *J. Urol.* **1996**, *155*, 361–367. [CrossRef]
6. Mayrhofer, G.; Schon-Hegrad, M.A. Ia Antigens in Rat Kidney, with Special Reference to Their Expression in Tubular Epithelium. *J. Exp. Med.* **1983**, *157*, 2097–2109. [CrossRef] [PubMed]
7. Wuthrich, R.P.; Glimcher, L.H.; Yui, M.A.; Jevnikar, A.M.; Dumas, S.E.; Kelley, V.E. MHC Class II, Antigen Presentation and Tumor Necrosis Factor in Renal Tubular Epithelial Cells. *Kidney Int.* **1990**, *37*, 783–792. [CrossRef] [PubMed]
8. Sinclair, G.D.; Wadgymar, A.; Halloran, P.F.; Delovitch, T.L. Graft-vs-Host Reactions Induce H-2 Class II Gene Transcription in Host Kidney Cells. *Immunogenetics* **1984**, *20*, 503–511. [CrossRef]
9. Benson, E.M.; Colvin, R.B.; Russell, P.S. Induction of IA Antigens in Murine Renal Transplants. *J. Immunol.* **1985**, *134*, 7–9.
10. Niemann-Masanek, U.; Mueller, A.; Yard, B.A.; Waldherr, R.; van der Woude, F.J. B7-1 (CD80) and B7-2 (CD 86) Expression in Human Tubular Epithelial Cells In Vivo and In Vitro. *Nephron* **2002**, *92*, 542–556. [CrossRef]
11. Wu, Q.; Jinde, K.; Endoh, M.; Sakai, H. Clinical Significance of Costimulatory Molecules CD80/CD86 Expression in IgA Nephropathy. *Kidney Int.* **2004**, *65*, 888–896. [CrossRef] [PubMed]
12. Den Haan, J.M.M.; Lehar, S.M.; Bevan, M.J. CD8+ but Not CD8− Dendritic Cells Cross-Prime Cytotoxic T Cells In Vivo. *J. Exp. Med.* **2000**, *192*, 1685–1696. [CrossRef] [PubMed]
13. Kovacsovics-Bankowski, M.; Clark, K.; Benacerraf, B.; Rock, K.L. Efficient Major Histocompatibility Complex Class I Presentation of Exogenous Antigen upon Phagocytosis by Macrophages. *Proc. Natl. Acad. Sci. USA* **1993**, *90*, 4942–4946. [CrossRef] [PubMed]
14. Cruz, F.M.; Colbert, J.D.; Merino, E.; Kriegsman, B.A.; Rock, K.L. The Biology and Underlying Mechanisms of Cross-Presentation of Exogenous Antigens on MHC-Imolecules. *Annu. Rev. Immunol.* **2017**, *35*, 149–176. [CrossRef]
15. Sigal, L.J.; Crotty, S.; Andino, R.; Rock, K.L. Cytotoxic T-Cell Immunity to Virus-Infected Nonhaematopoietic Cells Requires Presentation of Exogenous Antigen. *Nature* **1999**, *398*, 77–80. [CrossRef]
16. Huang, A.Y.; Golumbek, P.; Ahmadzadeh, M.; Jaffee, E.; Pardoll, D.; Levitsky, H. Role of Bone Marrow-Derived Cells in Presenting MHC Class I-Restricted Tumor Antigens. *Science* **1994**, *264*, 961–965. [CrossRef]
17. Game, D.S.; Lechler, R.I. Pathways of Allorecognition: Implications for Transplantation Tolerance. *Transpl. Immunol.* **2002**, *10*, 101–108. [CrossRef]
18. Ji, Q.; Castelli, L.; Goverman, J.M. MHC Class I-Restricted Myelin Epitopes are Cross-Presented by Tip-DCs That Promote Determinant Spreading to CD8+ T Cells. *Nat. Immunol.* **2013**, *14*, 254–261. [CrossRef]
19. Heath, W.R.; Belz, G.T.; Behrens, G.M.; Smith, C.M.; Forehan, S.P.; Parish, I.A.; Davey, G.M.; Wilson, N.S.; Carbone, F.R.; Villadangos, J.A. Cross-Presentation, Dendritic Cell Subsets, and the Generation of Immunity to Cellular Antigens. *Immunol. Rev.* **2004**, *199*, 9–26. [CrossRef]
20. Lohse, A.W.; Knolle, P.A.; Bilo, K.; Uhrig, A.; Waldmann, C.; Ibe, M.; Schmitt, E.; Gerken, G.; Meyer zum Büschenfelde, K.H. Antigen-Presenting Function and B7 Expression of Murine Sinusoidal Endothelial Cells and Kupffer Cells. *Gastroenterology* **1996**, *110*, 1175–1181. [CrossRef]
21. Horst, A.K.; Neumann, K.; Diehl, L.; Tiegs, G. Modulation of Liver Tolerance by Conventional and Nonconventional Antigen-Presenting Cells and Regulatory Immune Cells. *Cell. Mol. Immunol.* **2016**, *13*, 277–292. [CrossRef] [PubMed]
22. Limmer, A.; Ohl, J.; Kurts, C.; Ljunggren, H.G.; Reiss, Y.; Groettrup, M.; Momburg, F.; Arnold, B.; Knolle, P.A. Efficient Presentation of Exogenous Antigen by Liver Endothelial Cells to CD8+ T Cells Results in Antigen-Specific T-Cell Tolerance. *Nat. Med.* **2000**, *6*, 1348–1354. [CrossRef] [PubMed]
23. Limmer, A.; Ohl, J.; Wingender, G.; Berg, M.; Jüngerkes, F.; Schumak, B.; Djandji, D.; Scholz, K.; Klevenz, A.; Hegenbarth, S.; et al. Cross-Presentation of Oral Antigens by Liver Sinusoidal Endothelial Cells Leads to CD8 T Cell Tolerance. *Eur. J. Immunol.* **2005**, *35*, 2970–2981. [CrossRef] [PubMed]
24. Berg, M.; Wingender, G.; Djandji, D.; Hegenbarth, S.; Momburg, F.; Hämmerling, G.; Limmer, A.; Knolle, P. Cross-Presentation of Antigens from Apoptotic Tumor Cells by Liver Sinusoidal Endothelial Cells Leads to Tumor-Specific CD8+ T Cell Tolerance. *Eur J. Immunol.* **2006**, *36*, 2960–2970. [CrossRef]
25. Embgenbroich, M.; Burgdorf, S. Current Concepts of Antigen Cross-Presentation. *Front. Immunol.* **2018**, *9*, 1643. [CrossRef]
26. Burgdorf, S.; Lukacs-Kornek, V.; Kurts, C. The Mannose Receptor Mediates Uptake of Soluble but Not of Cell-Associated Antigen for Cross-Presentation. *J. Immunol.* **2006**, *176*, 6770–6776. [CrossRef]
27. Burgdorf, S.; Kautz, A.; Böhnert, V.; Knolle, P.A.; Kurts, C. Distinct Pathways of Antigen Uptake and Intracellular Routing in CD4 and CD8 T Cell Activation. *Science* **2007**, *316*, 612–616. [CrossRef]

28. Ackerman, A.L.; Giodini, A.; Cresswell, P. A Role for the Endoplasmic Reticulum Protein Retrotranslocation Machinery during Crosspresentation by Dendritic Cells. *Immunity* **2006**, *25*, 607–617. [CrossRef]
29. Imai, J.; Hasegawa, H.; Maruya, M.; Koyasu, S.; Yahara, I. Exogenous Antigens are Processed through the Endoplasmic Reticulum-Associated Degradation (ERAD) in Cross-Presentation by Dendritic Cells. *Int. Immunol.* **2005**, *17*, 45–53. [CrossRef]
30. Zehner, M.; Marschall, A.L.; Bos, E.; Schloetel, J.G.; Kreer, C.; Fehrenschild, D.; Limmer, A.; Ossendorp, F.; Lang, T.; Koster, A.J.; et al. The Translocon Protein Sec61 Mediates Antigen Transport from Endosomes in the Cytosol for Cross-Presentation to CD8(+) T Cells. *Immunity* **2015**, *42*, 850–863. [CrossRef]
31. Palmowski, M.J.; Gileadi, U.; Salio, M.; Gallimore, A.; Millrain, M.; James, E.; Addey, C.; Scott, D.; Dyson, J.; Simpson, E.; et al. Role of Immunoproteasomes in Cross-Presentation. *J. Immunol.* **2006**, *177*, 983–990. [CrossRef] [PubMed]
32. Kimura, H.; Caturegli, P.; Takahashi, M.; Suzuki, K. New Insights into the Function of the Immunoproteasome in Immune and Nonimmune Cells. *J. Immunol. Res.* **2015**, *2015*, 541984. [CrossRef] [PubMed]
33. Ackerman, A.L.; Kyritsis, C.; Tampé, R.; Cresswell, P. Early Phagosomes in Dendritic Cells Form a Cellular Compartment Sufficient for Cross Presentation of Exogenous Antigens. *Proc. Natl. Acad. Sci. USA* **2003**, *100*, 12889–12894. [CrossRef] [PubMed]
34. Saveanu, L.; Carroll, O.; Weimershaus, M.; Guermonprez, P.; Firat, E.; Lindo, V.; Greer, F.; Davoust, J.; Kratzer, R.; Keller, S.R.; et al. IRAP Identifies an Endosomal Compartment Required for MHC Class I Cross-Presentation. *Science* **2009**, *325*, 213–217. [CrossRef] [PubMed]
35. Savina, A.; Jancic, C.; Hugues, S.; Guermonprez, P.; Vargas, P.; Moura, I.C.; Lennon-Duménil, A.M.; Seabra, M.C.; Raposo, G.; Amigorena, S. NOX_2 Controls Phagosomal pH to Regulate Antigen Processing during Crosspresentation by Dendritic Cells. *Cell* **2006**, *126*, 205–218. [CrossRef]
36. Mantegazza, A.R.; Savina, A.; Vermeulen, M.; Pérez, L.; Geffner, J.; Hermine, O.; Rosenzweig, S.D.; Faure, F.; Amigorena, S. NADPH Oxidase Controls Phagosomal pH and Antigen Cross-Presentation in Human Dendritic Cells. *Blood* **2008**, *112*, 4712–4722. [CrossRef]
37. Bajema, I.M.; Wilhelmus, S.; Alpers, C.E.; Bruijn, J.A.; Colvin, R.B.; Cook, H.T.; D'Agati, V.D.; Ferrario, F.; Haas, M.; Charles, J.C.; et al. Revision of the ISN/RPS Classification for Lupus Nephritis: Modified NIH Activity and Chronicity Indices and Clarification of Definitions. *Kidney Int.* **2017**, *93*, 789–796. [CrossRef]
38. Summers, S.A.; Hoi, A.; Steinmetz, O.M.; O'Sullivan, K.M.; Ooi, J.D.; Odobasic, D.; Akira, S.; Kitching, A.R.; Holdsworth, S.R. TLR9 and TLR4 Are Required for the Development of Autoimmunity and Lupus Nephritis in Pristane Nephropathy. *J. Autoimmun.* **2010**, *35*, 291–298. [CrossRef]
39. Vinay, P.; Gougoux, A.; Lemieux, G. Isolation of a Pure Suspension of Rat Proximal Tubules. *Am. J. Physiol.* **1981**, *241*, F403–F411. [CrossRef]
40. Neumann, K.; Erben, U.; Kruse, N.; Wechsung, K.; Schumann, M.; Klugewitz, K.; Scheffold, A.; Kühl, A.A. Chemokine Transfer by Liver Sinusoidal Endothelial Cells Contributes to the Recruitment of CD4+ T Cells into the Murine Liver. *PLoS ONE* **2015**, *10*, e0123867. [CrossRef]
41. Nguyen, D.G.; Hildreth, J.E.K. Involvement of Macrophage Mannose Receptor in the Binding and Transmission of HIV by Macrophages. *Eur. J. Immunol.* **2003**, *33*, 483–493. [CrossRef] [PubMed]
42. Brunner, K.T.; Mauel, J.; Schindler, R. In Vitro Studies of Cell-Bound Immunity; Cloning Assay of the Cytotoxic Action of Sensitized Lymphoid Cells on Allogeneic Target Cells. *Immunology* **1966**, *11*, 499–506. [PubMed]
43. Krausgruber, T.; Fortelny, N.; Fife-Gernedl, V.; Senekowitsch, M.; Schuster, L.C.; Lercher, A.; Nemc, A.; Schmidl, C.; Rendeiro, A.F.; Bergthaler, A.; et al. Structural Cells Are Key Regulators of Organ-Specific Immune Responses. *Nature* **2020**, *583*, 296–302. [CrossRef]
44. Joffre, O.P.; Segura, E.; Savina, A.; Amigorena, S. Cross-Presentation by Dendritic Cells. *Nat. Rev. Immunol.* **2012**, *12*, 557–569. [CrossRef] [PubMed]
45. Knolle, P.A.; Limmer, A. Control of Immune Responses by Savenger Liver Endothelial Cells. *Swiss Med. Wkly.* **2003**, *133*, 501–506. [PubMed]
46. Martinez-Pomares, L. The Mannose Receptor. *J. Leukoc. Biol.* **2012**, *92*, 1177–1186. [CrossRef]
47. Sallusto, F.; Cella, M.; Danieli, C.; Lanzavecchia, A. Dendritic Cells Use Macropinocytosis and the Mannose Receptor to Concentrate Macromolecules in the Major Histocompatibility Complex Class II Compartment: Down-Regulation by Cytokines and Bacterial Products. *J. Exp. Med.* **1995**, *182*, 389–400. [CrossRef]
48. Wang, L.H.; Rothberg, K.G.; Anderson, R.G. Mis-Assembly of Clathrin Lattices on Endosomes Reveals a Regulatory Switch for Coated Pit Formation. *J. Cell Biol.* **1993**, *123*, 1107–1117. [CrossRef]
49. Betts, M.R.; Koup, R.A. Detection of T-Cell Degranulation: CD107a and B. *Methods Cell Biol.* **2004**, *75*, 497–512.
50. Alter, G.; Malenfant, J.M.; Altfeld, M. CD107a as a Functional Marker for the Identification of Natural Killer Cell Activity. *J. Immunol. Methods* **2004**, *294*, 15–22. [CrossRef]
51. Amir, E.A.D.; Davis, K.L.; Tadmor, M.D.; Simonds, E.; Levine, J.H.; Bendall, S.C.; Shenfeld, D.K.; Krishnaswamy, S.; Nolan, G.P.; Pe'er, D. ViSNE Enables Visualization of High Dimensional Single-Cell Data and Reveals Phenotypic Heterogeneity of Leukemia. *Nat. Biotechnol.* **2013**, *31*, 545–552. [CrossRef] [PubMed]
52. Kaczmarek, J.; Homsi, Y.; van Üüm, J.; Metzger, C.; Knolle, P.A.; Kolanus, W.; Lang, T.; Diehl, L. Liver Sinusoidal Endothelial Cell-Mediated CD8 T Cell Priming Depends on Co-Inhibitory Signal Integration over Time. *PLoS ONE* **2014**, *9*, e99574.

53. Diehl, L.; Schurich, A.; Grochtmann, R.; Hegenbarth, S.; Chen, L.; Knolle, P.A. Tolerogenic Maturation of Liver Sinusoidal Endothelial Cells Promotes B7-Homolog 1-Dependent CD8+ T Cell Tolerance. *Hepatology* **2008**, *47*, 296–305. [CrossRef] [PubMed]
54. Basler, M.; Mundt, S.; Bitzer, A.; Schmidt, C.; Groettrup, M. The Immunoproteasome: A Novel Drug Target for Autoimmune Diseases. *Clin. Exp. Rheumatol.* **2015**, *33*, S74–S79.
55. Bleackley, R.C. A Molecular View of Cytotoxic T Lymphocyte Induced Killing. *Biochem. Cell Biol.* **2005**, *83*, 747–751. [CrossRef]
56. Maier, T.; Güell, M.; Serrano, L. Correlation of mRNA and protein in complex biological samples. *FEBS Lett.* **2009**, *583*, 3966–3973. [CrossRef]
57. Vogel, C.; Marcotte, E.M. Insights into the regulation of protein abundance from proteomic and transcriptomic analyses. *Nat. Rev. Genet.* **2012**, *13*, 227–232. [CrossRef]
58. Engering, A.J.; Cella, M.; Fluitsma, D.; Brockhaus, M.; Hoefsmit, E.C.; Lanzavecchia, A.; Peters, J. The Mannose Receptor Functions as a High Capacity and Broad Specificity Antigen Receptor in Human Dendritic Cells. *Eur. J. Immunol.* **1997**, *27*, 2417–2425. [CrossRef]
59. Knolle, P.A.; Uhrig, A.; Hegenbarth, S.; Löser, E.; Schmitt, E.; Gerken, G.; Lohse, A.W. IL-10 down-Regulates T Cell Activation by Antigen-Presenting Liver Sinusoidal Endothelial Cells through Decreased Antigen Uptake via the Mannose Receptor and Lowered Surface Expression of Accessory Molecules. *Clin. Exp. Immunol.* **1998**, *114*, 427–433. [CrossRef]
60. Schurich, A.; Berg, M.; Stabenow, D.; Böttcher, J.; Kern, M.; Schild, H.-J.; Kurts, C.; Schuette, V.; Burgdorf, S.; Diehl, L.; et al. Dynamic Regulation of CD8 T Cell Tolerance Induction by Liver Sinusoidal Endothelial Cells. *J. Immunol.* **2010**, *184*, 4107–4114. [CrossRef]
61. Tolksdorf, F.; Mikulec, J.; Geers, B.; Endig, J.; Sprezyna, P.; Heukamp, L.C.; Knolle, P.A.; Kolanus, W.; Diehl, L. The PDL1-Inducible GTPase Arl4d Controls T Effector Function by Limiting IL-2 Production. *Sci. Rep.* **2018**, *8*, 16123. [CrossRef] [PubMed]
62. Alexopoulos, E.; Seron, D.; Hartley, R.B.; Cameron, J.S. Lupus Nephritis: Correlation of Interstitial Cells with Glomerular Function. *Kidney Int.* **1990**, *37*, 100–109. [CrossRef] [PubMed]
63. Winchester, R.; Wiesendanger, M.; Zhang, H.Z.; Steshenko, V.; Peterson, K.; Geraldino-Pardilla, L.; Ruiz-Vazquez, E.; D'Agati, V. Immunologic Characteristics of Intrarenal T Cells: Trafficking of Expanded CD8+ T Cell β-Chain Clonotypes in Progressive Lupus Nephritis. *Arthritis Rheum.* **2012**, *64*, 1589–1600. [CrossRef] [PubMed]
64. Couzi, L.; Merville, P.; Deminière, C.; Moreau, J.F.; Combe, C.; Pellegrin, J.L.; Viallard, J.F.; Blanco, P. Predominance of CD8+ T Lymphocytes among Periglomerular Infiltrating Cells and Link to the Prognosis of Class III and Class IV Lupus Nephritis. *Arthritis Rheum.* **2007**, *56*, 2362–2370. [CrossRef] [PubMed]
65. Arazi, A.; Rao, D.A.; Berthier, C.C.; Davidson, A.; Liu, Y.; Hoover, P.J.; Chicoine, A.; Eisenhaure, T.M.; Jonsson, A.H.; Li, S.; et al. The Immune Cell Landscape in Kidneys of Patients with Lupus Nephritis. *Nat. Immunol.* **2019**, *20*, 902–914. [CrossRef]
66. Chen, A.; Lee, K.; Guan, T.; He, J.C.; Schlondorff, D. Role of CD8+ T Cells in Crescentic Glomerulonephritis. *Nephrol. Dial. Transplant.* **2020**, *35*, 564–572. [CrossRef]
67. Anguiano, L.; Kain, R.; Anders, H.-J. The glomerular crescent: Triggers, evolution, resolution, and implications for therapy. *Curr. Opin. Nephrol. Hypertens.* **2020**, *29*, 302–309. [CrossRef]
68. Chang, J.; Eggenhuizen, P.; O'Sullivan, K.M.; Alikhan, M.A.; Holdsworth, S.R.; Ooi, J.D.; Kitching, A.R. CD8+ T Cells Effect Glomerular Injury in Experimental Anti-Myeloperoxidase GN. *J. Am. Soc. Nephrol.* **2017**, *28*, 47–55. [CrossRef]
69. Chen, A.; Lee, K.; D'Agati, V.D.; Wei, C.; Fu, J.; Guan, T.J.; He, J.C.; Schlondorff, D.; Agudo, J. Bowman's Capsule Provides a Protective Niche for Podocytes from Cytotoxic CD8+ T Cells. *J. Clin. Investig.* **2018**, *128*, 3413–3424. [CrossRef]
70. Goldwich, A.; Burkard, M.; Ölke, M.; Daniel, C.; Amann, K.; Hugo, C.; Kurts, C.; Steinkasserer, A.; Gessner, A. Podocytes Are Nonhematopoietic Professional Antigen-Presenting Cells. *J. Am. Soc. Nephrol.* **2013**, *24*, 906–916. [CrossRef]
71. Macconi, D.; Chiabrando, C.; Schiarea, S.; Aiello, S.; Cassis, L.; Gagliardini, E.; Noris, M.; Buelli, S.; Zoja, C.; Corna, D.; et al. Proteasomal Processing of Albumin by Renal Dendritic Cells Generates Antigenic Peptides. *J. Am. Soc. Nephrol.* **2009**, *20*, 123–130. [CrossRef] [PubMed]

Supplemental material

Antigen cross-presentation by murine proximal tubular epithelial cells induces cytotoxic and inflammatory CD8$^+$ T cells

Alexandra Linke[1]*, Hakan Cicek[1]*, Anne Müller[1,2], Catherine Meyer-Schwesinger[3] Simon Melderis[2,4], Thorsten Wiech[5], Claudia Wegscheid[1], Julius Ridder[1], Oliver M. Steinmetz[2,4], Linda Diehl[1,2], Gisa Tiegs[1,2], Katrin Neumann[1,2]

[1]Institute of Experimental Immunology and Hepatology, University Medical Center Hamburg-Eppendorf, Hamburg, Germany

[2]Hamburg Center for Translational Immunology, University Medical Center Hamburg-Eppendorf, Hamburg, Germany

[3]Institute of Cellular and Integrative Physiology, University Medical Center Hamburg-Eppendorf, Hamburg, Germany

[4]III. Medical Clinic, University Medical Center Hamburg-Eppendorf, Hamburg, Germany

[5]Institute of Pathology, University Medical Center Hamburg-Eppendorf, Hamburg, Germany

*equally contributed

Table of content: 1 table, 7 figures

Table S1. Sequences of the primer used for analysis of mRNA expression.

Target	Forward primer Reverse primer	Amplicon length	Annealing temperature
Actb	(fw) TATTGGCAACGAGCGGTTCC (rv) GGCATAGAGGTCTTTACGGATGTC	180 bp	60°C
Mrc1	(fw) GGAGGCTGATTACGAGCAGT (rv) TCCAGGTGAACCCCTCTGAA	87 bp	60°C
Sec61a1	(fw) TTCTGTGTCATCTTGCCGGA (rv) TGCCAAACAGGGGGATCTGA	124 bp	60°C
Sec61b	(fw) TGAGTGCTCGGCAACTTCAC (rv) GGGACAGGGCCCACTTTGA	282 bp	60°C
Sec61g	(fw) GCTCTCAATCCGCCATCCAA (rv) AGGACTCAGCCACCCACAAT	237 bp	60°C
Vcp	(fw) TGACCCTCATGGATGGCCTA (rv) TGTCAAAGCGACCAAATCGC	108 bp	60°C
Tap1	(fw) GGCTTACGTGGCTGAAGTCT (rv) AATGAGACAAGGTTGCCGCT	123 bp	60°C
Tap2	(fw) TGTGCAGACGACTTCATAGGG (rv) ATCTCCAGTTCTGTAGGGCCTG	199 bp	60°C
Lnpep	(fw) TTCGGCATGCTGTCATTCTT (rv) GAGTTTTGTCTGTGACCTC ATTG	99 bp	60°C
Cybb	(fw) GCCAGTGTGTCGAAATCTG (rv) AATTGTGTGGATGGCGGTGT	145 bp	60°C
Psmb8	(fw) GCCAAGGAGTGCAGGTTGTAT (rv) GCCGAGTCCCATTGTCATCT	184 bp	60°C

SUPPLEMENTAL FIGURE S1

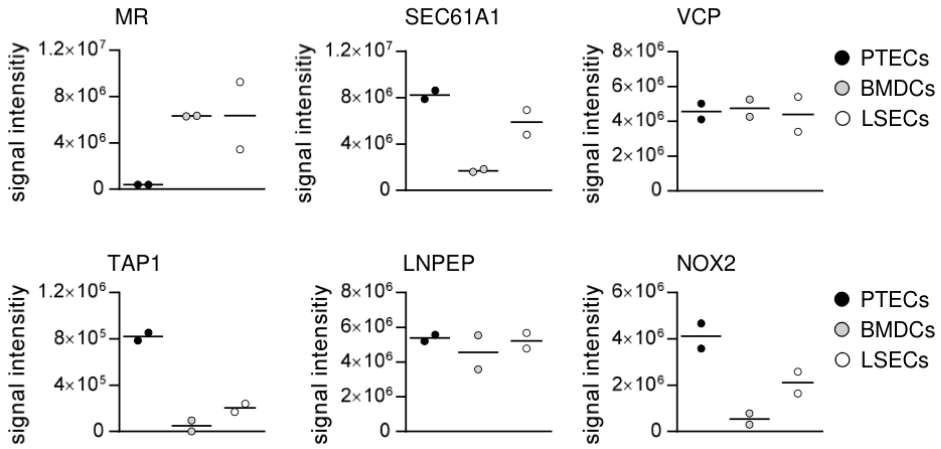

Supplemental Figure S1. Quantitative WB analysis. A densitometric analysis was done to otain realtive quantification of the analyzed proteins. Normalization was done in relation to the reference protein GAPDH. Medians show two experiments.

SUPPLEMENTAL FIGURE S2

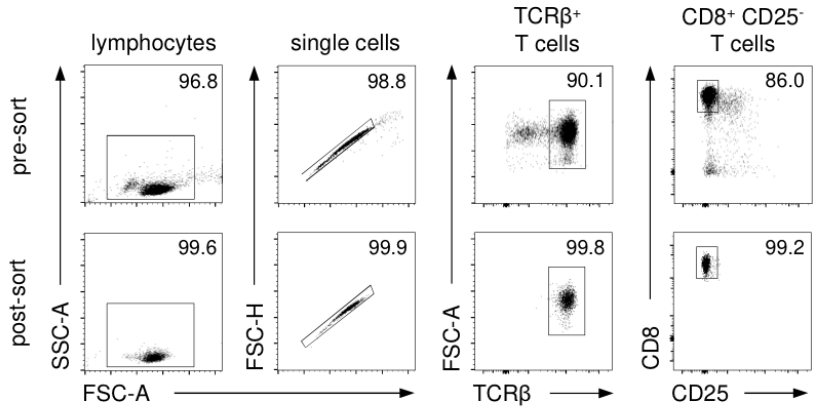

Supplemental Figure S2. Purity of isolated CD8⁺ T cells. $CD8^+$ $CD25^-$ T cells from spleen and lymph nodes of OT-I mice were enriched by MACS and purely isolated by FACS. Dot plots show representative data from at least 6 experiments.

SUPPLEMENTAL FIGURE S3

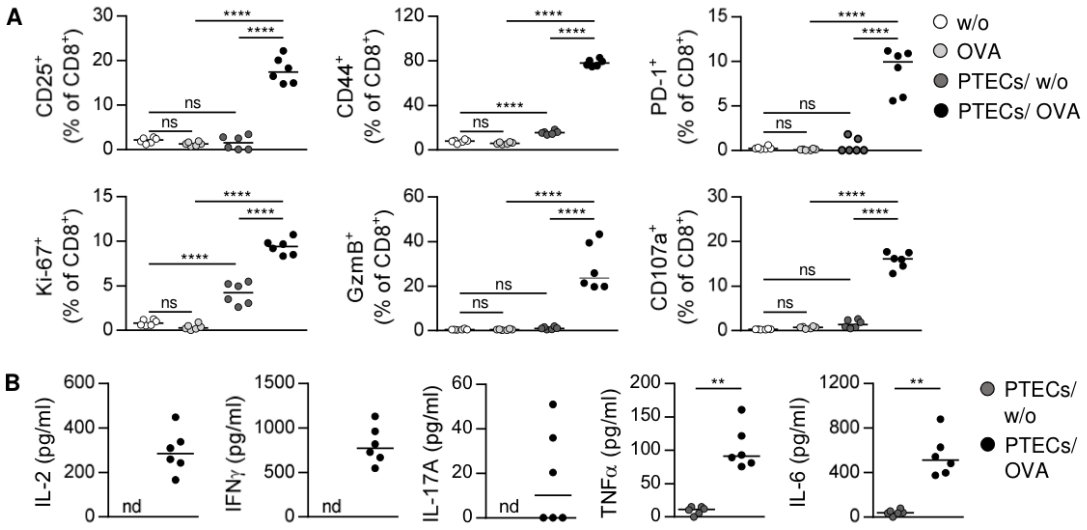

Supplemental Figure S3. Antigen-dependent activation of CD8⁺ T cells by PTECs after 5 days of co-culture. OVA-specific $CD8^+$ $CD25^-$ T cells were cultured with PTECs or alone in presence or absence of OVA protein for 5 days. (A) $CD8^+$ $TCR\beta^+$ T cells were stained for CD25, CD44, PD-1, Ki-67, CD107a and GzmB, and analyzed by flow cytometry. (B) Cytokine levels were determined in culture supernatants. Medians are shown from two experiments. *p< 0.05; ***p< 0.001; ****p< 0.0001; ns: not significant; nd: not detectable; w/o: without OVA.

SUPPLEMENTAL FIGURE S4

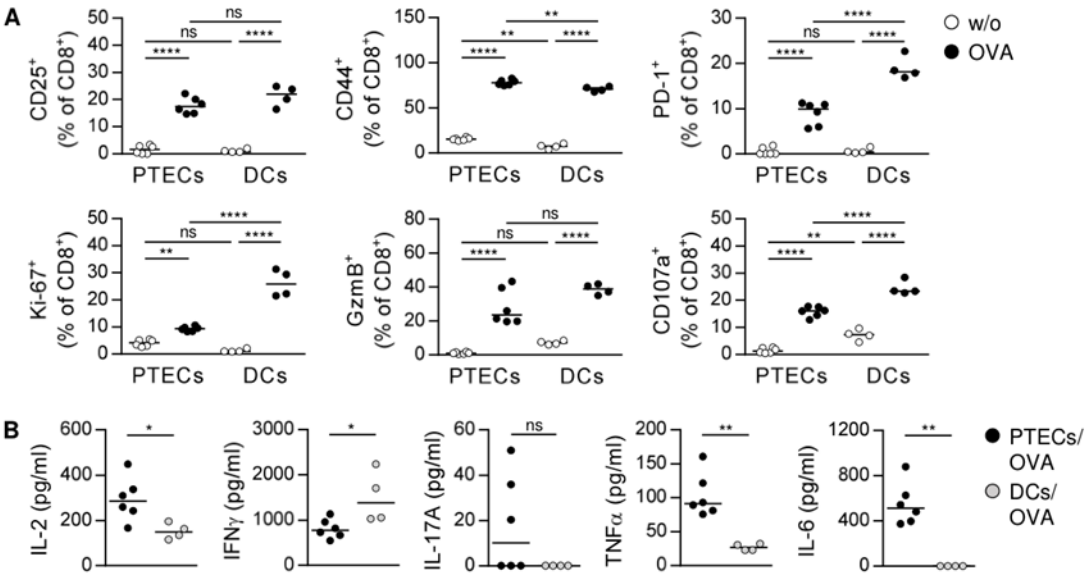

Supplemental Figure S4. Phenotype analysis of CD8⁺ T cells activated by PTECs or DCs after 5 days of co-culture. OVA-specific CD8⁺ CD25⁻ T cells were co-cultured with PTECs or DCs in presence or absence of OVA protein for 5 days. (A) CD8⁺ T cells were stained for CD25, CD44, PD-1, Ki-67, CD107a and GzmB, and analyzed by flow cytometry. (B) Cytokine levels were determined in co-culture supernatants. Means are shown from 1-2 experiments. *p< 0.05; **p< 0.01; ****p< 0.0001; ns: not significant; w/o: without OVA.

SUPPLEMENTAL FIGURE S5

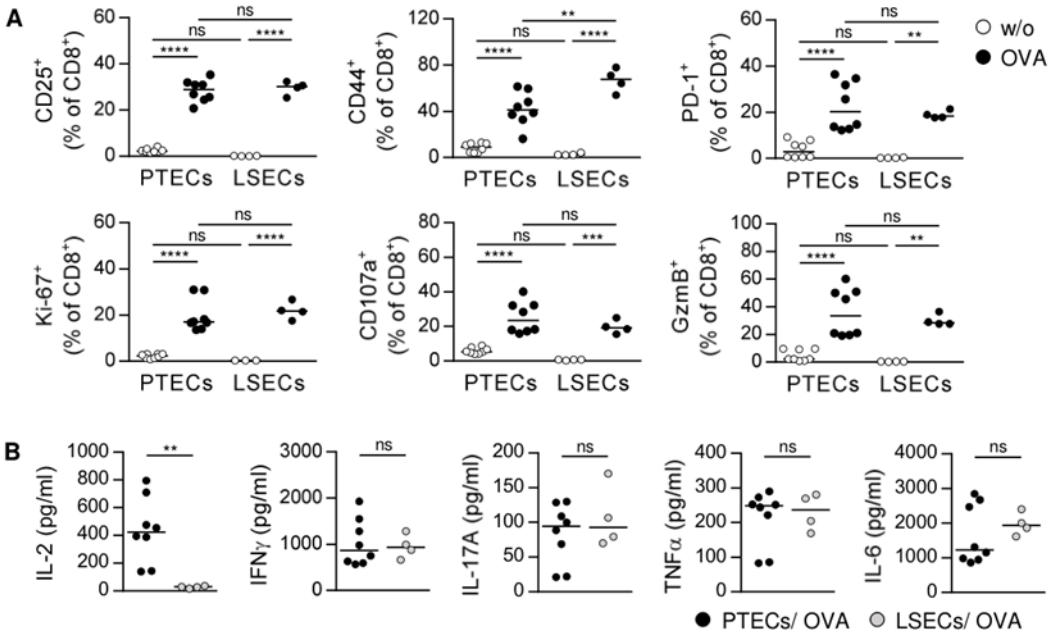

Supplemental Figure S5. Phenotype analysis of CD8⁺ T cells activated by PTECs or LSECs after 2.5 days of co-culture. OVA-specific CD8⁺ CD25⁻ T cells were co-cultured with PTECs or LSECs in presence or absence of OVA protein for 2.5 days. (A) CD8⁺ T cells were stained for CD25, CD44, PD-1, Ki-67, CD107a and GzmB, and analyzed by flow cytometry. (B) Cytokine levels were determined in co-culture supernatants. Means are shown from 1-2 experiments. **p< 0.01; ***p< 0.001; ****p< 0.0001; ns: not significant; w/o: without OVA.

SUPPLEMENTAL FIGURE S6

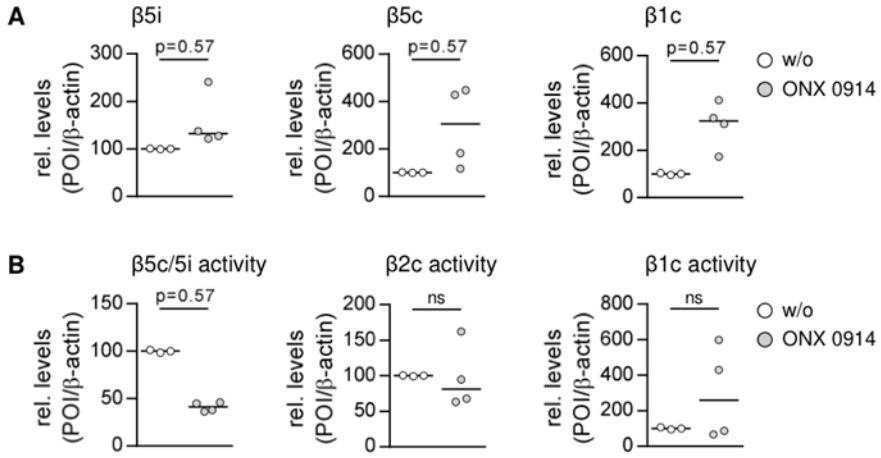

Supplemental Figure S6. Protein expression and catalytic activities of proteasome subunits. PTECs were treated with ONX 0914. (A) Protein expression of β5i, β5c and β1c was determined by WB analysis and depicted in relation to β-actin. (B) Activities of the different catalytic subunits were assessed by using ABPs. Medians of two experiments are shown. ns: not significant; w/o: without.

SUPPLEMENTAL FIGURE S7

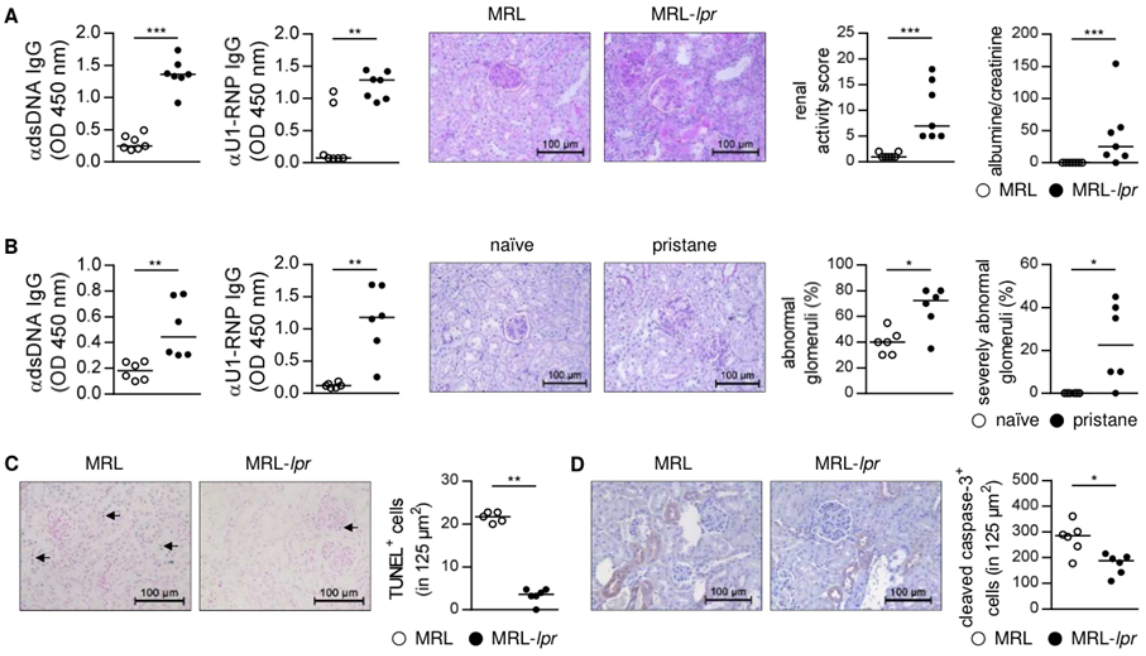

Supplemental Figure S7. Renal pathology in murine lupus nephritis models. (**A**) Lupus-prone MRL-*lpr* and MRL control mice were analyzed at an age of 15 weeks. Plasma autoantibody levels were determined by ELISA. PAS staining was performed in kidney sections. The activity score was assessed by a renal pathologist in a blinded manner. Albumin and creatinine levels were determined in urine. (**B**) WT mice were treated with pristane and analyzed 9 months later. Autoantibody levels were determined in plasma. PAS staining was performed in kidney sections. Frequencies of abnormal and severely abnormal glomeruli were assessed in a blinded manner. (**C**) Apoptotic cells were determined by TUNEL assay in kidney sections. (**D**) Numbers of cleaved caspase-3+ cells were assessed in kidney sections. Medians of 6-7 mice are shown. *p< 0.05; ***p< 0.001; αdsDNA: anti-double-stranded DNA; αU1-RNP: anti-U1-ribonucleoprotein.

2 Presentation of the publication

2.1 Introduction

The glomerulus as a signature structure of the kidney is the target of a group of inflammatory diseases leading to an impairment or even loss of kidney function. Among these kidney diseases, glomerulonephritis (GN) as a sterile inflammation of glomeruli and the surrounding interstitium and tubuli, is a leading cause of chronic kidney disease and the underlying disease of 10% to 15% of patients with end-stage renal disease (Kazi and Hashmi 2022). During GN, immune cells, such as dendritic cells (DCs) or T cells infiltrate the kidney and predominantly localize in the tubulointerstitium (Hu et al. 2016; Markovic-Lipkovski et al. 1990), close to tubular epithelial cells (TECs). TECs are involved in important tubular transport processes, with proximal tubular epithelial cells (PTECs) reabsorbing 85% of the ultrafiltrate fluid containing small proteins, glucose and other small molecules that can pass the glomerular filtration barrier (Yamaguchi et al. 2018). Since small proteins are highly concentrated during filtration, PTECs take up antigens at concentrations more than tenfold higher than in any other organ (Kurts et al. 2013). PTECs were described as non-professional antigen presenting cells (APCs), displaying low expression of the major histocompatibility complex class II (MHC–II) in healthy humans and naïve mice (Gastl et al. 1996; Hagerty and Allen 1992), which is enhanced during inflammation (van Dorp et al. 1993). Besides MHC-II, PTECs also express other molecules linked with APC function, such as the MHC-II histocompatibility gamma chain CD74 and the co-stimulatory molecules CD80 and CD86 (Breda et al. 2019). PTECs were shown to activate $CD4^+$ T cells antigen-specifically leading to $CD4^+$ T cell proliferation, interleukin (IL)-2 secretion and the production of the pro-inflammatory cytokines interferon γ (IFNγ) and tumor necrosis factor α (TNFα) (Breda et al. 2019). DCs as professional APCs not only activate $CD4^+$ T cells by presentation of exogenous, internalized antigen on MHC-II, they also activate $CD8^+$ T cells by cross-presentation of external antigen on MHC-I (Jung et al. 2002). For cross-presentation, external antigen is internalized by the APC into endosomes with low proteolytic activity (Fehres et al. 2014). The endosomes are alkalized by the NADPH oxidase (NOX)2 to avoid pH-dependent protease activation, which would result in impaired antigen cross-presentation (Embgenbroich and Burgdorf 2018). Especially mannose receptor (MR)-mediated endocytosis of exogenous antigens has been shown to be essential for cross-presentation (Burgdorf et al. 2007). The antigen can either be directly loaded onto recycled MHC-I in the phagosome (vacuolar pathway) or transported into the cytosol for further proteasomal degradation (endosome-to-cytosol pathway). The multimeric channel Sec61 plays a crucial role for the transport of antigens from the endosome into the cytosol and the energy for this transport derives from the ATPase valosin-containing protein (VCP) (Ackerman et al. 2006). Within the cytosol, proteasomal degradation leads to the

formation of antigen peptides. Antigen degradation for antigen peptide presentation on MHC-I was shown to be mediated by the constitutive but also by the immunoproteasome (Ferrington and Gregerson 2012; Palmowski et al. 2006), with the immunoproteasome being more potent in the activation of cytotoxic T cells (Groettrup et al. 2010; Kloetzel 2001). The resulting antigen peptides are transported back into the endosome *via* transporters associated with antigen processing (TAP) 1 and 2 (Huang et al. 1996). In the endosome, the peptides are further trimmed by the leucyl-cystinyl aminopeptidase (LNPEP) and then loaded onto MHC-I by the peptide loading complex (Embgenbroich and Burgdorf 2018; Fehres et al. 2014). Subsequently, the MHC-I molecule carrying the antigen peptide is transported to and incorporated into the cell's outer membrane for antigen presentation (Fehres et al. 2014) (Figure 1).

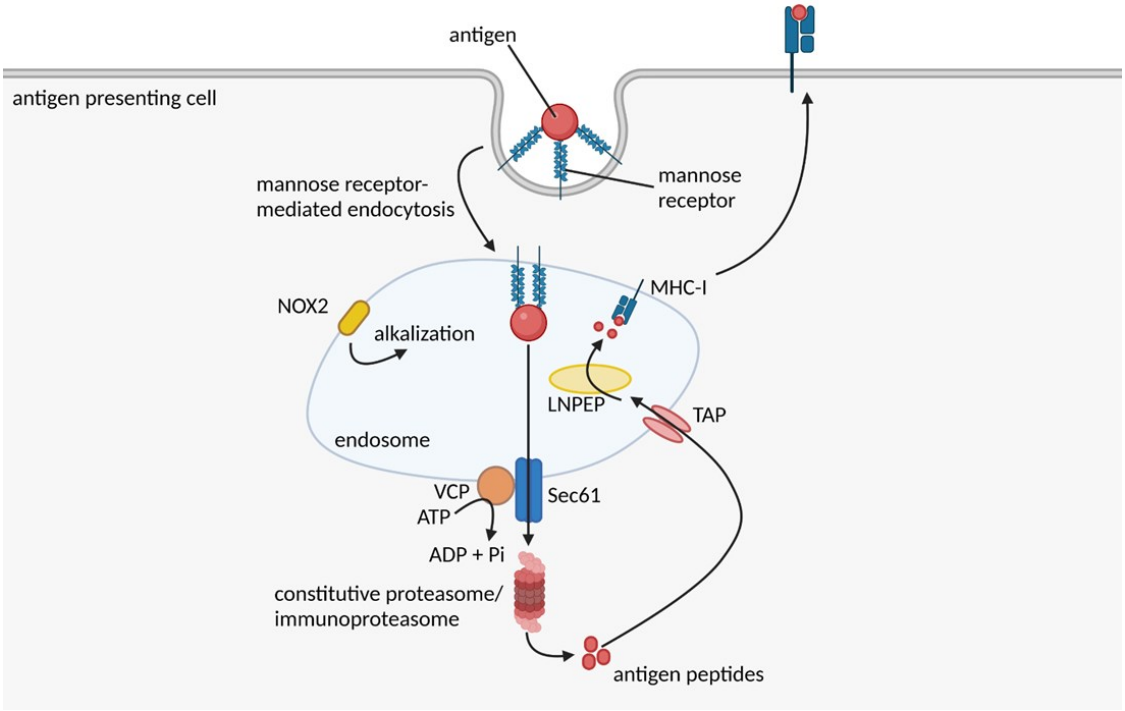

Figure 1: Schematic overview of the endosome-to-cytosol pathway of antigen cross-presentation. Exogenous antigen is internalized by mannose receptor-mediated endocytosis into the endosome. To avoid antigen degradation within the endosome, its milieu is alkalized by NOX2. The transport channel Sec61 translocates the antigen into the cytosol in an ATP-dependent manner. The energy for this translocation is provided by the ATPase VCP. In the cytosol, the antigen is degraded by the constitutive or immunoproteasome into antigen peptides. *Via* TAP, the antigen peptides are transported back into the endosome for further trimming by LNPEP. Afterwards, the peptides loading complex (not displayed in this figure) loads antigen peptides onto MHC-I molecules, which are transported to and incorporated into the cell's membrane for antigen presentation to $CD8^+$ T cells. NOX2: NADPH oxidase, VCP: valosin-containing protein, TAP: transporter associated with antigen processing, LNPEP: leucyl-cystinyl-aminopeptidase, MHC-I: major histocompatibility complex class I. Created with BioRender.com.

Via cross-presentation of external microbial or tumor antigens, $CD8^+$ T cell immunity in infectious or malignant diseases is acquired that is not restricted to endogenous-derived viral or tumor antigens (Fehres et al. 2014). Besides DCs, also non-professional APCs are capable of antigen cross-presentation. In the liver, which is permanently confronted with

food- and commensal bacteria-derived antigens from the intestine, non-parenchymal cells, such as liver sinusoidal endothelial cells (LSECs), have been shown to be potent cross-presenters of both cell-associated and soluble antigens (Ebrahimkhani et al. 2011; Lohse et al. 1996). Cross-presentation of exogenous antigen to $CD8^+$ T cells by LSECs leads to $CD8^+$ T cell tolerance both *in vitro* and *in vivo*, indicated by the loss of IFNγ and IL-2 production as well as reduced cytotoxicity (Limmer et al. 2000; Zheng and Tian 2019). If PTECs as non-professional APCs in the kidney are capable of antigen cross-presentation to $CD8^+$ T cells, is less clear. Therefore, this study aims at investigating the capacity of PTECs to cross-present soluble antigen to $CD8^+$ T cells *in vitro* and analyzes the phenotype and function of PTEC-activated $CD8^+$ T cells *in vitro*. This study further compares the phenotype of $CD8^+$ T cells activated by PTECs, LSECs or DCs *via* cross-presentation. Since one key effector function of activated $CD8^+$ T cells is to kill target cells, this study further analyzes the cytotoxic function of PTEC-activated $CD8^+$ T cells in a cytotoxicity assay and assesses induction of apoptosis in the nephritic kidneys of MRL/MpJ-*Fas*^{lpr} (MRL-*lpr*) and pristane-treated mice, both representing murine models of lupus nephritis (Freitas et al. 2017; Morse et al. 1982).

2.2 Material and Methods

This part describes the methods and murine models that I used during the study in more detail.

2.2.1 Animals and animal treatment

OT-I mice were used to isolate ovalbumin (OVA)-specific $CD8^+$ T cells. In these mice, all $CD8^+$ T cells contain a transgenic T cell receptor (TCR) recognizing the OVA peptide residues 257-264 ($OVA_{257-264}$) presented by MHC-I (Hogquist et al. 1994) and are, therefore, OVA-specific.

To induce systemic lupus erythematosus (SLE), C57BL/6 wild-type (WT) and *Cd8a*$^{-/-}$ mice were injected with 500 µL of pristane (2,6,10,14-Tetramethylpentadecane), a naturally occurring hydrocarbon oil inducing chronic inflammation upon injection (Reeves et al. 2010). Animals treated with pristane show clinical signs such as arthritis (Wooley et al. 1989), a lupus-like GN with deposition of antibodies and complement as well as pulmonary capillaritis (Chowdhary et al. 2007), anemia, and the production of autoantibodies (Reeves et al. 2010; Smith et al. 2007). The hydrocarbon induces an immune complex (IC) mediated GN with glomerular damage characterized by hypercellularity, mesangial expansion, crescent formation and interstitial mononuclear cell infiltration. Lupus-like GN and proteinuria begin 4 to 6 months after pristane injection (Freitas et al. 2017). WT mice develop mesangial expansion and hypercellularity within 7 months after pristane administration (Summers et al. 2014) and they develop a type III lupus nephritis after 9 and

a type IV lupus nephritis after 12 months (Kluger et al. 2016). Lupus autoantibodies targeted to nuclear components such as the U1 ribonucleoprotein (U1 RNP) develop within 4 to 6 months after SLE induction, while antibodies against double stranded deoxyribonucleic acid (dsDNA) emerge after 6 to 10 months (Reeves et al. 2010; Satoh et al. 2003). In our experiments, mice were analyzed 9 months after pristane injection after the beginning of autoantibody production and the type III lupus nephritis.

MRL/MpJ (MRL) and MRL-*lpr* mice have a diverse genetic background from standard inbred strains with a genome composed of LG (75%), AKR/J (12.6%), C3H (12.1%) and C57BL/6 (0.3%) (Peng et al. 1996). LG/J mice, which make up the largest proportion of the genetic background, exhibit autoantibodies, such as rheumatoid factor, as well as renal disease, including GN and interstitial nephritis (Peng et al. 1996). MRL-*lpr* mice are homozygous for the lymphoproliferation spontaneous mutation (*lpr*), a mutation in the gene of the TNF receptor superfamily member 6 (Fas-receptor) mediating apoptosis through the binding of its ligand, FasL (Nagata 1994). This mutation leads to the proliferation of aberrant T cells and to the development of systemic autoimmune disorders, such as a lupus-like disease and a generalized lymphadenopathy. MRL-*lpr* mice develop lupus-typical autoantibodies against nuclear components (Eisenberg et al. 1978). At 3 months of age, the MRL-*lpr* mice show increased levels of circulating ICs as well as a severe proliferative GN, while the MRL mice lacking the Fas^{lpr} mutation do not exhibit IC or GN development yet at this time point (Morse et al. 1982). Therefore, MRL mice showing the same genetic background as the MRL-*lpr* mice but lacking the Fas^{lpr} mutation were used as control mice. This model was used as a spontaneous model of GN in SLE. In both SLE models, the urinary albumin-to-creatinine ratio was measured to analyze proteinuria and kidney sections were stained with periodic acid-Schiff reagent to examine glomerular and tubular injury.

2.2.2 Co-Culture of OVA-specific $CD8^+$ T cells with PTECs or splenic DCs

PTECs were isolated from kidneys of WT mice and cultivated under sterile conditions in a CO_2 incubator at 37 °C with 5% CO_2 and saturated humidity. *Via* light microscopy, a monolayer of PTECs was visible after 3 days of cultivation. After 4 days, the PTECs were washed twice with 1 mL of RPMI and incubated in 1 mL/ well RPMI at 37 °C in the CO_2 incubator until T cell addition. After fluorescence-activated cell sorting (FACS) of OVA-specific naïve $CD25^-$ $CD8^+$ T lymphocytes from spleen and lymph nodes of OT-I mice, the T cells were counted and resuspended in RPMI with an adjusted cell count of 5 x 10^5 cells/ mL. RPMI was removed from the PTECs and 2.5 x 10^5 OVA-specific $CD8^+$ T cells were added to each well. The co-cultured cells were either treated with OVA (final concentration 500 µg/mL) or left without OVA. OVA-specific $CD8^+$ T cells were further cultured in the absence of PTECs with or without addition of OVA. After 2.5 or 5 days, $CD8^+$ T cells and

the co-culture supernatant were harvested for phenotype analysis *via* flow cytometry and LEGENDplex analysis to determine cytokine levels. OVA-specific $CD8^+$ T cells were further cultured with or without splenic DCs in the presence or absence of OVA and their phenotype was examined after 2.5 and 5 days.

2.2.3 Analysis of $CD8^+$ T cell phenotype by flow cytometry

Flow cytometry is a technique to measure physical and chemical properties of cells and particles. A cell suspension is injected into a flow cytometer and the fluidics system focuses the stream to a flow with one cell at a time through hydrodynamic focusing. Thereafter, the cell passes one or more beams of laser or arc lamp light. Light scattering or fluorescence emission, if the cell was labeled with a fluorochrome by the use of a fluorescently labeled antibody or a fluorescent dye, can be measured. The forward scatter is a measure for light diffraction in a flat angle up to 20°, its light is collected by the FSC and depends on the cell's size. Hence, the FCS can be used to distinguish between cell debris and living cells, for example. The side scatter is a measure for light refraction and can be detected at a 90° angle to the laser's excitation line by the side SSC. The SSC provides information about the granularity of cells. Consequently, a differentiation between different cell types by the combination of FSC and SSC signals is possible. Measuring the fluorescence at different wavelengths makes available quantitative and qualitative information about fluorochrome-labeled cell surface molecules or intracellular markers, such as cytokines or nucleic acids. Fluorochromes are dyes that can be excited by light energy, e.g. from a laser, and emit the energy at a longer wavelength. The process of emission is called fluorescence. It can be detected by fluorescence channels of the cytometer. These detectors are photomultiplier tubes and their specificity is controlled by optical filters, allowing specific wavelengths to pass, while blocking other wavelengths. The number of the detectors varies depending of the machine and its manufacturer. As soon as light is detected, a small current is generated at the detector. The voltage's amplitude is proportional to the number of light photons received by the detector. This voltage is then amplified and digitalized. Each detector provides a signal about one parameter, e.g. forward scatter, side scatter or fluorescence. For each parameter, one signal is referred to as one event or dot that can be seen on a digital plot. Consequently, each dot in the graph represents one event measurable for the parameter of interest. Since one flow cytometer can use several lasers to excite different fluorochromes, cells of a cell suspension can be stained with different fluorochromes and will be analyzed simultaneously (McKinnon 2019). The phenotype analysis in this study was performed with the LSR Fortessa™ Flow Cytometer and the FACS Diva software as well as the FlowJo software.

For the phenotype analysis of $CD8^+$ T cells *via* flow cytometry in this study, the T cells were stained with fluorochrome-linked antibodies directed against molecules on the cell surface, in the cytosol and in the nucleus after restimulation. Moreover, a fluorescent dye binding to amines was used to stain dead cells. Deviating from this staining procedure, the degranulation marker CD107a was stained during restimulation with phorbol 12-myristate 13-acetate (PMA) and ionomycin. CD107a belongs to the lysosomal-associated membrane glycoproteins (LAMPs), located in the membrane of cytosolic granules. During degranulation, the membrane of a cytosolic granule merges with the cell membrane, incorporating LAMPs into the plasma membrane. Consequently, LAMPs can be stained on the cell surface during degranulation. However, they become actively internalized into lysosomal compartments again, necessitating the staining during the activation period with application of monensin to neutralize the pH of lysosomal compartments to avoid loss of fluorescence signal (Betts and Koup 2004). Accordingly, CD107a was stained during re-stimulation. Each cell suspension was then analyzed *via* flow cytometry.

2.3 Results

2.3.1 PTECs express genes and proteins associated with antigen cross-presentation

To analyze whether renal epithelial cells and liver endothelial cells express mRNA of proteins associated with antigen cross-presentation, the expression of 10 genes connected with cross-presentation was examined, using the Log_2cpm, in epithelial cell adhesion molecule $(EpCAM)^+$ epithelial cells from kidneys of WT mice and in $CD31^+$ endothelial cells from the livers of WT mice. Renal epithelial cells strongly expressed the genes of VCP (*Vcp*), LNPEP (*Lnpep*), and Sec61 (*Sec61a1*, *Sec61b*, *Sec61g*). This analysis further showed substantial expression of genes of the MR (*Mrc1*) and of the large multifunctional peptidase (LMP7) (*Psmb8*), a subunit of the immunoproteasome (Ferrington and Gregerson 2012; Palmowski et al. 2006) in renal epithelial cells, while less expression of NOX2 (*Cybb*) and TAP1 and 2 (*Tap1*, *Tap2*) was observed. Liver endothelial cells showed higher expression of *Psmb8*, *Tap1* and *Mrc1* than renal epithelial cells, but less expression of *Sec61a1* and *Sec61b*. This analysis shows that total renal epithelial and hepatic endothelial cells express genes crucial for antigen cross-presentation. Furthermore, this study analyzed expression of these genes in cultured PTECs and compared it with these genes' expression by LSECs and bone marrow-derived DCs (BMDCs), both cell populations capable of antigen cross-presentation (Ebrahimkhani et al. 2011; Jung et al. 2002; Lohse et al. 1996). PTECs, BMDCs, and LSECs showed similar expression of *Sec61b*, *Sec61g*, *Lnpep*, and *Tap2*, whereas PTECs showed less expression of *Tap1* and *Mrc1* compared to LSECs and BMDCs. Moreover, LSECs showed higher expression of *Sec61a1* and *Vcp* than PTECs and BMDCs. Since this analysis shows expression of genes associated with antigen cross-

presentation in PTECs, this study further analyzed the expression of proteins crucial for cross-presentation in PTECs, compared to LSECs and BMDCs. All three cell populations similarly expressed VCP and LNPEP, while PTECs showed less expression of MR, but elevated expression of TAP1 and NOX2, compared to LSECs and BMDCs. Consequently, PTECs express genes and proteins associated with antigen cross-presentation.

2.3.2 Internalization of external antigen by PTECs *via* MR-mediated endocytosis

To analyze whether PTECs take up soluble external antigen, PTECs were cultured in the presence of fluorochrome-labeled OVA at 37°C and 4°C for 1, 2 and 4 hours with subsequent flow cytometry analysis of OVA^+ PTECs. The frequency of OVA^+ PTECs increased over time after culture at 37°C, whereas it was low after incubation at 4°C. To analyze whether PTECs internalize exogenous antigen in an MR-dependent manner, PTECs were further cultured with fluorochrome-labeled OVA in the presence of mannan, which binds to the MR with high affinity, thereby leading to competitive MR inhibition (Burgdorf et al. 2006). The frequency of OVA^+ PTECs decreased after pre-treatment with mannan compared to PTECs not treated with mannan. Pre-treatment of PTECs with D-galactose not binding to the MR (Nguyen and Hildreth 2003), did not reduce OVA internalization by PTECs. Furthermore, PTECs were cultured in the presence of the clathrin-specific inhibitor chlorpromazine (Vercauteren et al. 2010) to analyze the effect of inhibition of endocytosis on antigen uptake. This treatment resulted in a reduced frequency of OVA^+ PTECs compared to PTECs not pre-treated with chlorpromazine. Consequently, PTECs take up external soluble antigen *via* MR-mediated endocytosis.

2.3.3 PTECs induce a pro-inflammatory and cytotoxic phenotype in $CD8^+$ T cells that is similar to the phenotype induced by DCs *via* antigen cross-presentation

To assess antigen-dependent activation of $CD8^+$ T cells by PTECs, OVA-specific $CD25^-$ $CD8^+$ T cells were co-cultured with PTECs in the presence or absence of OVA and their phenotype was analyzed by flow cytometry after 2.5 days. After co-culture of OVA-specific $CD8^+$ T cells with PTECs in the presence of OVA, $CD8^+$ T cells expressed the activation markers CD44, CD25 and PD-1 and the proliferation marker Ki-67, indicating T cell activation and proliferation. These PTEC-activated $CD8^+$ T cells further expressed GzmB and the degranulation marker CD107a, indicating a cytotoxic phenotype. Moreover, the $CD8^+$ T cells secreted IL-2 as well as the pro-inflammatory cytokines IFNγ, TNFα, IL-17A, and IL-6, indicating a pro-inflammatory phenotype. In contrast, the controls only containing $CD8^+$ T cells with or without OVA or with PTECs but in the absence of OVA did not show $CD8^+$ T cell activation nor induction of the other assessed markers. After 5 days of co-culture with PTECs in the presence of OVA, the $CD8^+$ T cells still showed activation and proliferation as well as a cytotoxic and pro-inflammatory phenotype. Splenic DCs as

professional APCs induced a similar phenotype after 2.5 and 5 days of co-culture with $CD8^+$ T cells in the presence of OVA. viSNE analysis revealed similar $CD8^+$ T cell clusters after activation by PTECs and DCs, with one cluster co-expressing CD44 and Ki-67 and another cluster co-expressing CD25 and CD-44, while another big cluster showed mono-expression of CD44. Both DC- and PTEC-activated $CD8^+$ T cells showed a degranulated T cell cluster, containing $CD107a^+$ $GzmB^{low}$ $CD8^+$ T cells, and a not degranulated T cell cluster containing $CD107a^{low}$ $GzmB^+$ $CD8^+$ T cells. In comparison to DC-activated $CD8^+$ T cells, the frequency of PTEC-activated $CD8^+$ T cells expressing CD25 or Ki-67 was lower, but the frequency of $CD107a^+$ $CD8^+$ T cells was higher. PTECs induced elevated IL-2 and IL-6-secretion compared to DCs, whereas DCs induced more secretion of IFNγ. The frequency of $CD44^+$, $PD\text{-}1^+$, $GzmB^+$ $CD8^+$ T cells as well as cytokine levels of IL-17A and TNFα were similar after co-culture with PTECs or DCs. Consequently, both PTECs and DCs induced a similar pro-inflammatory and cytotoxic phenotype in $CD8^+$ T cells through antigen cross-presentation, while DCs induced stronger activation and proliferation.

2.3.4 In contrast to PTECs, LSECs induce a tolerogenic phenotype in $CD8^+$ T cells *via* antigen cross-presentation

The phenotype of PTEC-activated $CD8^+$ T cells was compared to the one of LSEC-activated $CD8^+$ T cells after 2.5 and 5 days of co-culture. After 2.5 days of co-culture, the phenotype induced by PTECs and LSECs was similar, showing activation, proliferation and expression of markers associated with cytotoxicity and inflammation. In comparison to PTECs inducing high secretion of IL-2, LSECs induced low secretion of IL-2. After 5 days of co-culture, PTEC-activated $CD8^+$ T cells still showed a cytotoxic and pro-inflammatory phenotype. Interestingly, LSEC-activated $CD8^+$ T cells were still activated but did not express markers associated with cytotoxicity or Ki-67. Moreover, the level of IFNγ was strongly reduced while IL-2 was not detectable any more. The frequency of LSEC-activated $CD8^+$ T cells expressing the activation marker and co-inhibitory receptor PD-1 was elevated compared to PTEC-activated $CD8^+$ T cells after 5 days of co-culture. Since LSECs were shown to induce $CD8^+$ T cell inhibition *via* PD-1/ PD-L1 interaction in the liver (Diehl et al. 2008; Iwai et al. 2003) and the PD-1/PD-L1 pathway was shown to play an immune-regulatory role in GN (Neumann et al. 2019), PTECs and LSECs were further analyzed for their expression of the co-inhibitory ligand PD-L1. During T cell activation, interaction of the co-stimulatory ligand CD80 or CD86 with the co-stimulatory receptor CD28 constitutes the second T cell activation signal (Kambayashi and Laufer 2014; Tamura et al. 1996). Since $CD8^+$ T cells were activated after co-culture with either PTECs or LSECs and OVA, the expression of CD80 and CD86 was analyzed in PTECs and LSECs. LSECs showed more expression of the co-inhibitory ligand PD-L1, whereas PTECs, but not LSECs, expressed the co-stimulatory molecules CD80 and CD86. Consequently, the phenotype of $CD8^+$ T cells after

2.5 days of co-culture with PTECs or LSECs was similar showing activation, proliferation and expression of cytotoxicity- and inflammation-associated cytokines. After 5 days, however, a striking difference of phenotype induced by PTECs or LSECs in $CD8^+$ T cells *via* cross-presentation was revealed, showing a maintained pro-inflammatory and cytotoxic phenotype in PTEC-activated $CD8^+$ T cells, but a tolerogenic phenotype in LSEC-activated $CD8^+$ T cells with reduced IFNγ expression and loss of GzmB expression.

2.3.5 An active (immuno) proteasome is needed for antigen cross-presentation by PTECs

The immunoproteasome and its subunit LMP7 were shown to play a role in antigen cross-presentation (Ferrington and Gregerson 2012; Palmowski et al. 2006). To analyze whether PTECs express this proteasomal subunit, gene expression analysis of *Psmb8* and the referring protein LMP7 was performed. PTECs expressed *Psmb8* and LMP7, but LMP7 expression was lower compared to LSECs and BMDCs. To assess the role of LMP7 in antigen cross-presentation, PTECs were pre-treated for 4 hours with the LMP7- inhibitor ONX 0914 before co-culture with OVA-specific $CD8^+$ T cells. $CD8^+$ T cells only co-cultured with PTECs in the presence or absence of ONX 0914 did not show activation or induction of cytotoxicity- or inflammation-associated markers. In the co-culture with presence of OVA, the pre-treatment of PTECs with ONX 0914 led to reduced expression of the assessed markers for activation, proliferation, cytotoxicity and reduced secretion of inflammatory cytokines by $CD8^+$ T cells in comparison to the co-culture without pre-treatment of PTECs with ONX 0914. Moreover, expression of subunits of the immunoproteasome (β5i/LMP7) and of the constitutive proteasome (β5c, β1c, β2c) were analyzed in PTECs after treatment with ONX 0914 to assess the specificity of proteasome inhibition mediated by ONX 0914. ONX 0914-treated PTECs showed a higher protein accumulation of the subunits β5i, β5c, and β1c compared to untreated PTECs. With the use of activity-based probes (ABPs), which bind to active proteasomal subunits (Gan et al. 2019), a reduced activity of β5i and β5c in ONX 0914-treated compared to untreated PTECs was shown, indicating that ONX 0914 inhibited a subunit of the immunoproteasome, but also a subunit of the constitutive proteasome.

2.3.5 PTEC-activated $CD8^+$ T cells have cytolytic function

Since PTEC-activated $CD8^+$ T cells showed a cytotoxic phenotype with expression of GzmB and CD107a, their capacity to exert cytotoxic function was analyzed in a cytotoxicity assay using allogeneic P815 cells as target cells (Talmage et al. 1977). The P815 cells were allogeneic, thus, the TCR of the $CD8^+$ T cells recognized their foreign MHC molecules leading to $CD8^+$ T cell activation and killing of target cells. P815 cells were cultured with PTEC-activated $CD8^+$ T cells for 4 hours. For controls, P815 cells were cultured with $CD8^+$

T cells cultured alone with or without OVA or in the presence of PTECs but absence of OVA. After 4 hours, the cells were stained for CD8a and with 7-amino actinomycin D (7-AAD), a viability dye that penetrates dead cells but is excluded by living cells (Johnson et al. 2013). Subsequently, the frequency of 7-AAD$^+$ CD8$^-$ P815 cells was determined by flow cytometry to assess P815 cell killing. CD8$^+$ T cells cultured without PTECs in the presence or absence of OVA did not induce P815 cell death. The frequency of 7-AAD$^+$ P815 cells increased after addition of CD8$^+$ T cells co-cultured with PTECs and showed substantial increase after addition of CD8$^+$ T cells co-cultured with PTECs in the presence of OVA. Consequently, the cytotoxicity assay showed that PTEC-activated CD8$^+$ T cells exerted cytotoxicity.

2.3.6 CD8$^+$ T cells induce cell death in murine lupus nephritis

CD8$^+$ T cell phenotype and renal localization of CD8$^+$ T cells were further analyzed in murine lupus nephritis. Both MRL-*lpr* and pristane-treated mice showed lupus-typical autoantibody production and renal damage characteristic of lupus nephritis. Serial CD8/ CD3 staining of renal tissue sections revealed elevated numbers of CD8$^+$ T cells in the nephritic contrasted to healthy kidneys in both murine lupus nephritis models. In the inflamed kidneys, CD8$^+$ T cells predominantly localized in the tubulointerstitium, while glomerular CD8$^+$ T cell numbers were low. Phenotype analysis of renal CD8$^+$ T cells in these murine models showed a higher frequency of GzmB$^+$, CD107a$^+$, IFNγ$^+$, and IL-17A$^+$ CD8$^+$ T cells in nephritic compared to healthy kidneys, indicating a pro-inflammatory and cytotoxic phenotype of CD8$^+$ T cells in lupus nephritis. Since killing of target cells is a key function of cytotoxic CD8$^+$ T cells, analysis of renal apoptotic cell death by Terminal deoxynucleotidyl transferase dUTP nick end labeling (TUNEL) (Moore et al. 2021) and cleaved caspase-3 (Goping et al. 2003) staining was performed and showed an increase of apoptotic cell numbers in pristane-treated compared to control mice. The number of TUNEL$^+$ and cleaved caspase-3$^+$ cells was reduced in *Cd8a*$^{-/-}$ compared to nephritic WT mice. Mostly TECs were TUNEL$^+$, while mainly PTECs and glomerular cells were cleaved caspase-3$^+$. In contrast, MRL-*lpr* mice showed reduced numbers of TUNEL$^+$ and cleaved caspase-3$^+$ renal cells compared to MRL mice.

2.4 Discussion

During GN, T cells, among other immune cells, infiltrate the kidney (Kurts et al. 2013; Markovic-Lipkovski et al. 1990) and CD4$^+$ T cells were shown to mediate both pro-inflammatory (Azadegan-Dehkordi et al. 2015; Palmer and Weaver 2010; Schmidt et al. 2018) and immune-regulatory (Alikhan et al. 2018; Neumann et al. 2019; Neumann and Tiegs 2021; Ooi et al. 2011; Paust et al. 2011; Tipping and Holdsworth 2006; Turner et al. 2010) functions. The role of kidney-intrinsic cells in immune-mediated GN is less clear. PTECs were shown to be non-professional APCs in the kidney with expression of CD80

and CD86, able to activate $CD4^+$ T cells antigen-specifically, thereby leading to a pro-inflammatory $CD4^+$ T cell phenotype (Breda et al. 2019). This study shows that PTECs are capable of cross-presenting exogenous, soluble antigen to $CD8^+$ T cells *in vitro*, thereby inducing a cytotoxic and pro-inflammatory $CD8^+$ T cell phenotype. Expression analysis showed that PTECs express mRNA and proteins of the antigen cross-presentation machinery depicted in Figure 1, indicating that they, similarly as BMDCs and LSECs, possess the proteins necessary to present external, internalized antigen to $CD8^+$ T cells *via* MHC-I. This study further shows that PTECs express LMP7, a proteasomal subunit specific of the immunoproteasome, which has been implicated to be crucial for antigen cross-presentation (Ferrington and Gregerson 2012; Palmowski et al. 2006). Moreover, inhibition experiments targeting the MR and clathrin-molecules showed that the external antigen becomes internalized in PTECs *via* MR-mediated endocytosis, which was shown to be essential for cross-presentation (Burgdorf et al. 2007). Subsequent co-cultures of PTECs with OVA-specific $CD8^+$ T cells in the presence of the antigen OVA showed $CD8^+$ T cell activation, proliferation and the expression of cytotoxicity- and inflammation-associated molecules. This result was not observed in the control groups only containing $CD8^+$ T cells cultured alone with or without OVA or in the presence of PTECs without OVA, indicating that PTECs are able to present exogenous antigen to $CD8^+$ T cells. Consequently, PTECs are not only able to present exogenous antigen *via* MHC-II to $CD4^+$ T cells, thereby leading to activation and a pro-inflammatory $CD4^+$ T cell response (Breda et al. 2019). They are also able to cross-present external antigen *via* MHC-I to $CD8^+$ T cells, leading to activation and induction of a pro-inflammatory and cytotoxic phenotype in $CD8^+$ T cells. Pre-treatment of PTECs with the LMP7-inhibitor ONX 0914 resulted in less activation of $CD8^+$ T cells, indicating that antigen cross-presentation depended on active LMP7, a subunit of the immunoproteasome (Ferrington and Gregerson 2012). However, this study identified not only LMP7, but also β5c, a subunit of the conventional proteasome (Ferrington and Gregerson 2012), to be target of ONX 0914, indicating that PTECS might involve both the immunoproteasome and the constitutive proteasome for antigen cross-presentation.

DCs are professional APCs with the capacity of antigen cross-presentation, thereby mediating $CD8^+$ T cell immunity in infectious or malignant diseases (Fehres et al. 2014). In the liver, which is permanently confronted with intestinal food- and commensal bacteria-derived antigens, LSECs, among other non-parenchymal cells, were shown to be potent cross-presenters of both cell-associated and soluble antigens (Ebrahimkhani et al. 2011; Lohse et al. 1996). Cross-presentation of external antigen to $CD8^+$ T cells by LSECs leads to $CD8^+$ T cell tolerance, indicated by the loss of IFNγ and IL-2 production as well as reduced cytotoxicity, hence, reduced effector functions (Limmer et al. 2000; Zheng and Tian 2019). In co-culture experiments in this study, PTECs, DCs and LSECs induced $CD8^+$ T cell

activation, proliferation and expression of markers associated with cytotoxicity and inflammation within 2.5 days of co-culture. Moreover, PTEC-activated $CD8^+$ T cells exerted cytotoxicity in this study. After 5 days, this phenotype was preserved by PTEC- and DC-activated $CD8^+$ T cells, whereas LSEC-activated $CD8^+$ T cells showed a tolerogenic phenotype with reduced IFNγ and GzmB expression and no detection of IL-2. Since IL-2 was induced in low amounts after 2.5 days of co-culture with LSECs and not detectable after 5 days of co-culture, the $CD8^+$ T cells might have consumed the low amount of IL-2 in an autocrine way during their activation. While these findings are consistent with the literature depicting tolerance induction by LSECs (Limmer et al. 2000; Zheng and Tian 2019), they show that PTECs rather induce $CD8^+$ T cell immunity and effector function similarly as DCs than immune tolerance. LSECs in this study induced a higher expression of PD-1 in $CD8^+$ T cells than PTECs and showed higher expression of PD-L1 than PTECs. This agrees with the literature showing LSECs to induce $CD8^+$ T cell tolerance *via* the PD-L1/PD-1 pathway (Diehl et al. 2008; Iwai et al. 2003), which might explain why LSECs induced a tolerogenic phenotype in $CD8^+$ T cells. For full $CD8^+$ T cell activation, antigen presentation *via* MHC-I and recognition by the TCR and further co-stimulatory signals are necessary (Hamilos 1989). One co-stimulatory signal is provided by the interaction of the co-stimulatory receptor CD28 on the T cell with its ligands CD80 or CD86, expressed on activated professional APCs (Kambayashi and Laufer 2014). Eventually, this leads to autocrine IL-2 production and clonal expansion of the antigen-specific T cell. Consequently, the higher expression of the co-stimulatory molecules CD80 and CD86 by PTECs than by LSECs further explains why PTECs induce $CD8^+$ T cell activation rather than tolerance. This might further explain the low induction of IL-2 by LSECs. These findings depict that organ-specific non-professional APCs induce different $CD8^+$ T cell responses *via* cross-presentation. While LSECs as non-parenchymal hepatic cells induce immune tolerance, PTECs seem to be involved in induction of inflammation and cytotoxicity in the kidney.

This study further showed mainly tubulointerstitial localization of renal $CD8^+$ T cells in murine lupus nephritis. In the tubulointerstitium, $CD8^+$ T cells are localized close to PTECs. This arises the question of whether PTECs cross-present antigen deriving from the ultrafiltrate to $CD8^+$ T cells situated in the tubulointerstitium during GN *in vivo*. During GN with destruction of the filtration barrier, antigens might be liberated into the ultrafiltrate and be internalized by PTECs and presented to tubulointerstitial T cells. Since proteinuria is a clinical sign of GN, the presence of proteins, such as albumin, in the ultrafiltrate might lead to antigen uptake by PTECs. PTECs were shown to generate antigenic peptides from autologous albumin. This antigenic peptide was further processed by DCs, which then presented the processed antigen *via* MHC-I to $CD8^+$ T cells leading to $CD8^+$ T cell activation *in vitro* (Macconi et al. 2009). If PTECs are directly able to cross-present albumin-derived

antigens to tubulointerstitial $CD8^+$ T cells, thereby leading to $CD8^+$ T cell immunity in the kidney without antigen transmission to renal DCs, needs further investigation.

Moreover, TUNEL and cleaved caspase-3 staining showed apoptosis of TECs in the presence of $CD8^+$ T cells in pristane-induced lupus nephritis, which was reduced in *Cd8a*$^{-/-}$ mice. Consequently, $CD8^+$ T cells seem to be involved in the induction of apoptosis in renal cells in lupus nephritis. Since mainly PTECs were cleaved caspase-3^+ and this study shows PTECs to induce cytotoxic $CD8^+$ T cells *via* antigen cross-presentation, PTECs might become a target of the cytotoxic $CD8^+$ T cells that they induce or of kidney-infiltrating cytotoxic $CD8^+$ T cells activated in renal lymph nodes. In MRL-*lpr* mice lacking the Fas/FasL pathway for induction of cell death, the number of $TUNEL^+$ cells was reduced compared to control mice, indicating that the Fas/FasL pathway plays a role in cell death induction in lupus nephritis. If PTECs contribute to disease pathology by induction of inflammatory and cytotoxic $CD8^+$ T cells, which then initiate apoptosis in autoimmune GN *in vivo*, needs further investigation. The potential role of cross-presentation by PTECs and the phenotype of $CD8^+$ T cells induced by cross-presentation and found in lupus nephritis in this study are illustrated in Figure 2.

To find out if PTECs are capable of activating $CD8^+$ T cells *in vivo*, future experiments using mice in which PTECs selectively express OVA with induction of GN as well as adoptive transfer of OVA-specific $CD8^+$ T cells to these mice with subsequent phenotype and function analysis of the transferred $CD8^+$ T cells are necessary.

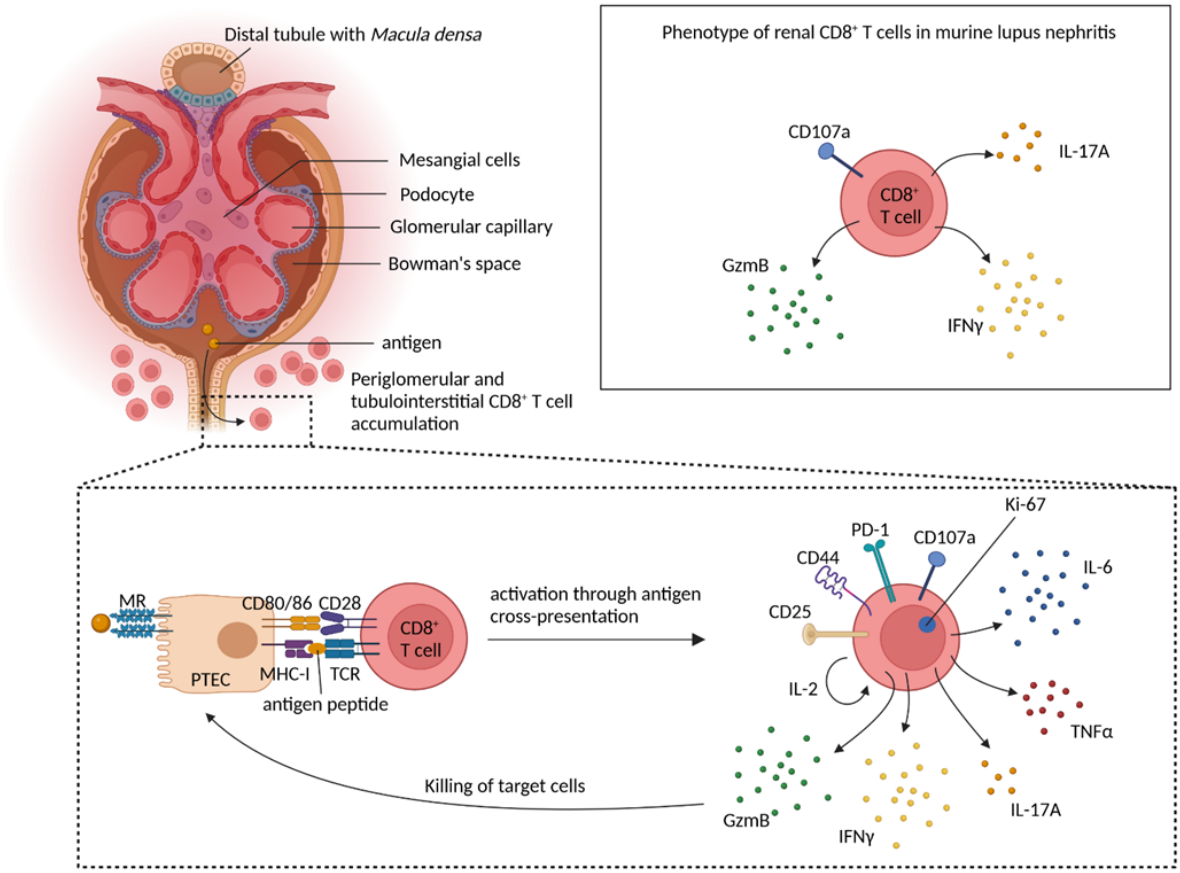

Figure 2: Potential pathogenic role of antigen cross-presentation of ultrafiltrate-derived antigens by PTECs and the phenotype of PTEC-activated CD8⁺ T cells and renal CD8⁺ T cells in murine lupus nephritis. The renal corpuscule, containing the glomerulus and Bowman's capsule, is shown. PTECs might internalize ultrafiltrate-derived antigens by mannose receptor-mediated endocytosis and process it by proteins crucial for antigen cross-presentation (antigen processing is not shown). PTECs then cross-present antigen peptides to renal CD8⁺ T cells, thereby inducing CT8⁺ T cell activation, proliferation and expression of cytotoxicity-associated and pro-inflammatory molecules. *Via* GzmB, CD8⁺ T cells mediate killing of their target cells, e.g. PTECs. Moreover, the phenotype of renal CD8⁺ T cells in murine lupus nephritis of MRL-*lpr* and pristane-treated mice is depicted. MR: mannose receptor; PTEC: Proximal Tubular Epithelial Cell. Created with BioRender.com.

3 References

Ackerman AL, Giodini A, Cresswell P (2006) A Role for the Endoplasmic Reticulum Protein Retrotranslocation Machinery during Crosspresentation by Dendritic Cells. Immunity 25(4): 607–617.

Alikhan MA, Huynh M, Kitching AR, Ooi JD (2018) Regulatory T cells in renal disease. Clin. Transl. Immunol. 7(1): 1–14.

Azadegan-Dehkordi F, Bagheri N, Shirzad H, Rafieian-Kopaei M (2015) The role of Th1 and Th17 cells in glomerulonephritis. J. Nephropathol. 4(2): 32–37.

Betts MR, Koup RA (2004) Detection of T-cell degranulation: CD107a and b. Methods Cell Biol. 2004(75): 497–512.

Breda PC, Wiech T, Meyer-Schwesinger C, Grahammer F, Huber T, Panzer U, Tiegs G, Neumann K (2019) Renal proximal tubular epithelial cells exert immunomodulatory function by driving inflammatory $CD4^+$ T cell responses. Am. J. Physiol. Physiol. 317(1): F77–F89.

Burgdorf S, Lukacs-Kornek V, Kurts C (2006) The Mannose Receptor Mediates Uptake of Soluble but Not of Cell-Associated Antigen for Cross-Presentation. J. Immunol. 176(11): 6770–6776.

Burgdorf S, Kautz A, Böhnert V, Knolle PA, Kurts C (2007) Distinct Pathways of Antigen Uptake. Science 612(316): 612–616.

Chowdhary VR, Grande JP, Luthra HS, David CS (2007) Characterization of haemorrhagic pulmonary capillaritis: Another manifestation of Pristane-induced lupus. Rheumatology 46(9): 1405–1410.

Diehl L, Schurich A, Grochtmann R, Hegenbarth S, Chen L, Knolle PA (2008) Tolerogenic Maturation of Liver Sinusoidal Endothelial Cells Promotes B7-Homolog 1-Dependent $CD8^+$ T Cell Tolerance. Hepatology 47(1): 296–305.

Ebrahimkhani MR, Mohar I, Crispe IN (2011) Cross-Presentation of Antigen by Diverse Subsets of Liver Cells. Hepatology 54(4): 1379–1387.

Eisenberg RA, Tan EM, Dixon FJ (1978) Presence of Anti-Sm Reactivity in autoimmune mouse strains. J. Exp. Med. 147: 582–587.

Embgenbroich M, Burgdorf S (2018) Current concepts of antigen cross-presentation. Front. Immunol. 9(1643): 1–10.

Fehres CM, Unger WWJ, Garcia-Vallejo JJ, van Kooyk Y (2014) Understanding the biology of antigen cross-presentation for the design of vaccines against cancer. Front. Immunol. 5(149): 1–10.

Ferrington DA, Gregerson DS (2012) Immunoproteasomes: Structure, function, and antigen presentation. Prog. Mol. Biol. Transl. Sci. 109: 75–112.

Freitas EC, de Oliveira MS, Monticielo OA (2017) Pristane-induced lupus: considerations on this experimental model. Clin. Rheumatol. 36(11). Clinical Rheumatology: 2403–2414.

Gan J, Leestemaker Y, Sapmaz A, Ovaa H (2019) Highlighting the proteasome: Using fluorescence to visualize proteasome activity and distribution. Front. Mol. Biosci. 6(MAR): 1–8.

Gastl G, Ebert T, Finstad CL, Sheinfeld J, Gomahr A, Aulitzky W, Bander NH (1996) Major histocompatibility complex class I and class II expression in renal cell carcinoma and modulation by interferon gamma. J. Urol. 155(1): 361–7.

Goping IS, Barry M, Liston P, Sawchuk T, Constantinescu G, Michalak KM, Shostak I, Roberts DL, Hunter AM, Korneluk R, Bleackley RC (2003) Granzyme B-induced apoptosis requires both direct caspase activation and relief of caspase inhibition. Immunity 18(3): 355–365.

Groettrup M, Kirk CJ, Basler M (2010) Proteasomes in immune cells: More than peptide producers? Nat. Rev. Immunol. 10(1). Nature Publishing Group: 73–78.

Hagerty DT, Allen PM (1992) Processing and presentation of self and foreign antigens by the renal proximal tubule. J. Immunol. 148(8): 2324–30.

Hamilos DL (1989) Antigen presenting cells. Immunol. Res. 8(2): 98–117.

Hogquist KA, Jameson SC, Heath WR, Howard JL, Bevan MJ, Carbone FR (1994) T cell receptor antagonist peptides induce positive selection. Cell 76(1): 17–27.

Hu SY, Jia XY, Li JN, Zheng X, Ao J, Liu G, Cui Z, Zhao MH (2016) T cell infiltration is associated with kidney injury in patients with anti-glomerular basement membrane disease. Sci. China Life Sci. 59(12): 1282–1289.

Huang AYC, Bruce AT, Pardoll DM, Levitsky HI (1996) In vivo cross-priming of MHC class I-restricted antigens requires the TAP transporter. Immunity 4(4): 349–355.

Iwai Y, Terawaki S, Ikegawa M, Okazaki T, Honjo T (2003) PD-1 Inhibits Antiviral Immunity at the Effector Phase in the Liver The Journal of Experimental Medicine. J. Exp. Med. 198(1): 39–50.

Johnson S, Nguyen V, Coder D (2013) Assessment of cell viability. Curr. Protoc. Cytom. (SUPPL.64): 1–26.

Jung S, Unutmaz D, Wong P, Sano G-I, De Ios Santos K, Sparwasser T, Wu S, Vuthoori S, Ko K, Zavala F, Pamer EG, Littman DR, Lang RA (2002) In vivo depletion of CD11c+ dendritic cells abrogates priming of CD8+ T cells by exogenous cell-associated antigens. Immunity 17(2): 211–220.

Kambayashi T, Laufer TM (2014) Atypical MHC class II-expressing antigen-presenting cells: Can anything replace a dendritic cell? Nat. Rev. Immunol. 14(11): 719–730.

Kazi AM, Hashmi MF (2022) *Glomerulonephritis*. Treasure Island: StatPearls Publishing

Kloetzel PM (2001) Antigen processing by the proteasome. Nat. Rev. Mol. Cell Biol. 2(3): 179–187.

Kluger MA, Melderis S, Nosko A, Goerke B, Luig M, Meyer MC, Turner JE, Meyer-Schwesinger C, Wegscheid C, Tiegs G, Stahl RAK, Panzer U, Steinmetz OM (2016) Treg17 cells are programmed by Stat3 to suppress Th17 responses in systemic lupus. Kidney Int. 89(1). Elsevier Inc: 158–166.

Kurts C, Panzer U, Anders HJ, Rees AJ (2013) The immune system and kidney disease: Basic concepts and clinical implications. Nat. Rev. Immunol. 13(10): 738–753.

Limmer A, Ohl J, Kurts C, Ljunggren HG, Reiss Y, Groettrup M, Momburg F, Arnold B, Knolle PA (2000) Efficient presentation of exogenous antigen by liver endothelial cells to CD8+ T cells results in antigen-specific T-cell tolerance. Nat. Med. 6(12): 1348–1354.

Lohse AW, Knolle PA, Bilo K, Uhrig A, Waldmann C, Ibe M, Schmitt E, Gerken G, Buschenfelde KHMZ (1996) Antigen-presenting function and B7 expression of murine sinusoidal endothelial cells and Kupffer cells. Gastroenterology 110(4): 1175–1181.

Macconi D, Chiabrando C, Schiarea S, Aiello S, Cassis L, Gagliardini E, Noris M, Buelli S, Zoja C, Corna D, Mele C, Fanelli R, Remuzzi G, Benigni A (2009) Proteasomal processing of albumin by renal dendritic cells generates antigenic peptides. J Am Soc

Nephrol. 20: 123–30.

Markovic-Lipkovski J, Müller CA, Risler T, Bohle A, Müller GA (1990) Association of glomerular and inerstitial mononuclear leukocytes with different forms of glomerulonephritis. Nephrol. Dial. Transplant. 5(1): 10–17.

McKinnon KM (2019) Flow cytometry: An Overview. Curr. Protoc. Immunol. 120(1): 5.1.1-5.1.11.

Moore CL, Savenka A V., Basnakian AG (2021) Tunel assay: A powerful tool for kidney injury evaluation. Int. J. Mol. Sci. 22(1): 1–17.

Morse HC, Davidson WF, Yetter RA, Murphy ED, Roths J, Coffman RL (1982) Abnormalities induced by the mutant gene lpr : expansion of a unique lymphocyte subset . J. Immunol. 129(6): 2612–2615.

Nagata S (1994) Mutations in the Fas antigen gene in lpr mice. Immunology 6(1): 3–8.

Neumann K, Tiegs G (2021) Immune regulation in renal inflammation. Cell Tissue Res. 385(2). Springer Berlin Heidelberg: 305–322.

Neumann K, Ostmann A, Breda PC, Ochel A, Tacke F, Paust HJ, Panzer U, Tiegs G (2019) The co-inhibitory molecule PD-L1 contributes to regulatory T cell-mediated protection in murine crescentic glomerulonephritis. Sci. Rep. 9(1): 1–13.

Nguyen DG, Hildreth JEK (2003) Involvement of macrophage mannose receptor in the binding and transmission of HIV by macrophage. Eur. J. Immunol. 33(2): 483–493.

Ooi JD, Snelgrove SL, Engel DR, Hochheiser K, Ludwig-Portugall I, Nozaki Y, O'Sullivan KM, Hickey MJ, Holdsworth SR, Kurts C, Kitching AR (2011) Endogenous foxp3+ T-regulatory cells suppress anti-glomerular basement membrane nephritis. Kidney Int. 79(9). Elsevier Masson SAS: 977–986.

Palmer MT, Weaver CT (2010) Autoimmunity: Increasing suspects in the CD4 + T cell lineup. Nat. Immunol. 11(1). Nature Publishing Group: 36–40.

Palmowski MJ, Gileadi U, Salio M, Gallimore A, Millrain M, James E, Addey C, Scott D, Dyson J, Simpson E, Cerundolo V (2006) Role of Immunoproteasomes in Cross-Presentation. J. Immunol. 177(2): 983–990.

Paust HJ, Ostmann A, Erhardt A, Turner JE, Velden J, Mittrücker HW, Sparwasser T, Panzer U, Tiegs G (2011) Regulatory T cells control the Th1 immune response in murine crescentic glomerulonephritis. Kidney Int. 80(2): 154–164.

Peng SL, Madaio MP, Craft J (1996) Systemic autoimmunity in LG/J mice. Immunol. Lett. 53(2–3): 153–155.

Reeves WH, Lee PY, Weinstein JS, Satoh M, Lu L (2010) Induction of autoimmunity by pristane and other naturally occuring hydrocarbons. Trends Immunol. 30(9): 455–464.

Satoh M, Kuroda Y, Yoshida H, Behney KM, Mizutani A, Akaogi J, Nacionales DC, Lorenson TD, Rosenbauer RJ, Reeves WH (2003) Induction of lupus autoantibodies by adjuvants. J. Autoimmun. 21(1): 1–9.

Schmidt T, Luebbe J, Paust HJ, Panzer U (2018) Mechanisms and functions of IL-17 signaling in renal autoimmune diseases. Mol. Immunol. 104(September). Elsevier: 90–99.

Smith DL, Dong X, Du S, Oh MS, Singh RR, Voskuhl RR (2007) A female preponderance for chemically induced lupus in SJL/J mice. Clin. Immunol. 122(1): 101–107.

Summers SA, Odobasic D, Khouri MB, Steinmetz OM, Yang Y, Holdsworth SR, Kitching AR (2014) Endogenous interleukin (IL)-17A promotes pristane-induced systemic

autoimmunity and lupus nephritis induced by pristane. Clin. Exp. Immunol. 176(3): 341–350.

Talmage DW, Woolnough JA, Hemmingsen H, Lopez L, Lafferty KJ (1977) Activation of cytotoxic T cells by nonstimulating tumor cells and spleen cell factor(s). Proc. Natl. Acad. Sci. U. S. A. 74(10): 4610–4614.

Tamura N, Ishii N, Nakazawa M, Nagoya M, Yoshinari M, Amano T, Nakazima H, Minami M (1996) Requirement of CD80 and CD86 Molecules for Antigen Presentation by Eosinophils. Scand. J. Immunol. 44(3): 229–238.

Tipping PG, Holdsworth SR (2006) T cells in crescentic glomerulonephritis. J. Am. Soc. Nephrol. 17(5): 1253–1263.

Turner JE, Paust HJ, Steinmetz OM, Peters A, Riedel JH, Erhardt A, Wegscheid C, Velden J, Fehr S, Mittrücker HW, Tiegs G, Stahl RAK, Panzer U (2010) CCR6 recruits regulatory T cells and Th17 cells to the kidney in glomerulonephritis. J. Am. Soc. Nephrol. 21(6): 974–985.

van Dorp WT, van Wieringen PAM, Marselis-Jonges E, Gruggeman CA, Daha M, van Es LA, van der Woude FJ (1993) CMV directly enhances MHC Class I and Intercellular Adhesion Molecule-1 Expression on cultured Proximal Tubular Epithelial Cells. Transplantation 55(6): 1367–1371.

Vercauteren D, Vandenbroucke RE, Jones AT, Rejman J, Demeester J, De Smedt SC, Sanders NN, Braeckmans K (2010) The use of inhibitors to study endocytic pathways of gene carriers: Optimization and pitfalls. Mol. Ther. 18(3): 561–569.

Wooley PH, Seibold JR, Whalen JD, Chapdelaine JM (1989) Pristane-induced arthritis. the immunologic and genetic features of an experimental murine model of autoimmune disease. Arthritis Rheum. 32(8): 1022–1030.

Yamaguchi T, Higa N, Okura N, Matsumoto A, Hermawan I, Yamashiro T, Suzuki T, Toma C (2018) Characterizing interactions of Leptospira interrogans with proximal renal tubule epithelial cells. BMC Microbiol. 18(1). BMC Microbiology: 1–11.

Zheng M, Tian Z (2019) Liver-Mediated Adaptive Immune Tolerance. Front. Immunol. 10(2525): 1–12.

4 Summary

During GN, T cells infiltrate the kidney and accumulate mainly in the tubulointerstitium close to PTECs. Different T cell subsets were shown to have either a pro-inflammatory or an immune-regulatory role in GN. The role of PTECs as kidney-intrinsic cells in GN pathology is less clear. PTECs were shown to be non-professional APCs in the kidney, expressing proteins connected with antigen presentation, such as MHC-II, CD74 and the co-stimulatory molecules CD80 and CD86 and presented exogenous antigen to $CD4^+$ T cells *via* MHC-II, thereby activating them and leading to pro-inflammatory cytokine expression in $CD4^+$ T cells (Breda et al. 2019). If PTECs are able to cross-present exogenous antigen *via* MHC-I, thereby leading to $CD8^+$ T cell activation, is less clear. This study analyzes the capacity of PTECs for antigen cross-presentation in *in vitro* co-culture experiments with OVA-specific $CD8^+$ T cells using OVA as antigen. Gene and protein expression analysis showed that PTECs express proteins crucial for antigen cross-presentation, such as the MR, the transport channel Sec61, the ATPase VCP, LMP7, a subunit of the immunoproteasome, and TAP transporters. Moreover, using MR- and clathrin-inhibitors, this study reveals that PTECs internalize antigen *via* MR-dependent endocytosis. $CD8^+$ T cells were co-cultured with PTECs, LSECs as non-professional APCs from liver or DCs as professional APCs and the phenotype of $CD8^+$ T cells was analyzed after 2.5 and 5 days of co-culture. After 2.5 days, all three APC types induced T cell activation, proliferation and expression of pro-inflammatory and cytotoxicity-associated molecules. After 5 days, the phenotype of DC- and PTEC-activated $CD8^+$ T cells was similar to the phenotype after 2.5 days, whereas LSEC-activated $CD8^+$ T cells did not proliferate, lost IL-2 expression and showed strongly reduced expression of IFNγ or GzmB. Consequently, while LSECs contribute to a tolerogenic phenotype of $CD8^+$ T cells *via* antigen cross-presentation, PTECs induce inflammation and cytotoxicity. A cytotoxicity assay showed that PTEC-activated $CD8^+$ T cells exerted cytotoxic function by killing allogeneic target cells. Pre-treatment of PTECs with the LMP7 inhibitor ONX 0914 reduced $CD8^+$ T cell activation by PTECs. Moreover, proteasomal subunit expression analysis and the use of ABPs revealed that PTECs use both the immunoproteasome and the constitutive proteasome for antigen cross-presentation. CD8/CD3 staining of renal tissue showed mainly tubulointerstitial and only minor intraglomerular $CD8^+$ T cell accumulation in murine lupus nephritis. Apoptotic cell death was analyzed in nephritic kidneys of pristane-treated mice and showed especially TECs to be apoptotic. The absence of $CD8^+$ T cells in *Cd8*$^{-/-}$ mice resulted in reduced apoptosis of TECs. In MRL-*lpr* mice lacking the Fas/FasL pathway for induction of cell death, the number of apoptotic cells was reduced compared to control mice. In a nutshell, this study depicts PTECs to be potent antigen cross-presenters, thereby inducing inflammatory and cytotoxic $CD8^+$ T cells.

Moreover, $CD8^+$ T cells are shown to mediate induction of tubular apoptosis in murine lupus nephritis.

5 Zusammenfassung

T Zellen infiltrieren in der GN die Niere und akkumulieren insbesondere im Tubulointerstitium nah an PTECs. Es konnte gezeigt werden, dass verschiedene T Zell Subtypen eine pro-inflammatorische oder immunregulatorische Rolle in der GN spielen. Die Rolle von PTECs als nierenintrinsische Zellen in der GN Pathologie ist unklar. Es konnte gezeigt werden, dass PTECs nicht-professionelle APCs in der Niere sind, die Proteine, welche mit Antigenpräsentation assoziiert sind, wie MHC-II, CD74 und die ko-stimulatorischen Moleküle CD80 und CD86, exprimieren. Zudem präsentierten PTECs exogenes Antigen an $CD4^+$ T Zellen *via* MHC-II, was zur T Zell Aktivierung und Expression inflammatorischer und zytotoxischer Moleküle durch $CD4^+$ T Zellen führte (Breda et al. 2019). Ob PTECs in der Lage sind, Antigene über MHC-I kreuz zu präsentieren und damit $CD8^+$ T Zellen zu aktivieren, ist unklar. Diese Studie analysiert die Kapazität von PTECs zur Antigen Kreuzpräsentation in *in vitro* Ko-Kulturen mit OVA-spezifischen $CD8^+$ T Zellen und OVA als Antigen. Gen- und Proteinexpressionsanalysen zeigten, dass PTECs Proteine, die wichtig für Kreuzpräsentation sind, wie MR, den Transportkanal Sec61, die ATPase VCP, die Immunoproteasom-Untereinheit LMP7 und TAP Transporter, exprimieren. Darüber hinaus zeigt diese Studie durch Anwendung von MR- und Clathrin-Inhibitoren, dass PTECs Antigen in einer MR-abhängigen Endozytose internalisieren. $CD8^+$ T Zellen wurden mit PTECs, LSECs als nicht-professionellen APCs aus der Leber und DCs als professionellen APCs ko-kultiviert und der Phänotyp der $CD8^+$ T Zellen wurde nach 2,5 und 5 Tagen analysiert. Nach 2,5 Tagen induzierten alle drei APC Typen T Zell Aktivierung, Proliferation und Expression pro-inflammatorischer und Zytotoxizität-assoziierter Moleküle. Nach 5 Tagen war der Phänotyp PTEC- und DC-aktivierter $CD8^+$ T Zellen ähnlich wie nach 2,5 Tagen, wohingegen LSEC-aktivierte $CD8^+$ T Zellen nicht mehr proliferierten, kein IL-2 mehr sezernierten und eine starke Reduktion der Expression von IFNγ und GzmB zeigten. Folglich tragen LSECs durch Antigen Kreuzpräsentation zu einem tolerogenen Phänotyp von $CD8^+$ T Zellen bei, wohingegen PTECs Inflammation und Zytotoxizität induzieren. Ein Zytotoxizitätsassay zeigte, dass PTEC-aktivierte $CD8^+$ T Zellen allogene Zielzellen abtöten. Eine Vorbehandlung der PTECs mit dem LMP7 Inhibitor ONX 0914 reduzierte $CD8^+$ T Zell Aktivierung. Zudem zeigten Analyse der Expression von Proteasomuntereinheiten sowie die Anwendung von ABPs, dass PTECs sowohl das Immunoproteasom als auch das konstitutive Proteasom für Antigen Kreuzpräsentation nutzen. Apoptose wurde in entzündeten Nieren Pristan-behandelter Mäuse analysiert und es zeigte sich, dass vor allem TECs apoptotisch sind in der Lupusnephritis. Das Fehlen von $CD8^+$ T Zellen in *Cd8*$^{-/-}$ Mäusen resultierte in reduzierter Apoptose von TECs. In MRL-*lpr* Mäusen, in denen der Fas/FasL Weg zur Induktion von Apoptose fehlt, war die Zahl TUNEL positiver Zellen im Vergleich zu Kontrollmäusen reduziert. Zusammenfassend zeigt diese Studie, dass PTECs

potente Antigen kreuzpräsentierende Zellen sind und dadurch inflammatorische und zytotoxische $CD8^+$ T Zellen induzieren. Darüber hinaus zeigt die Studie, dass $CD8^+$ T Zellen in der Lupusnephritis tubuläre Apoptose induzieren.

6 Explanation of the contribution to the publication

This project was designed under the leadership of Prof. Gisa Tiegs and Dr. Katrin Neumann and performed in close consultation of all authors.

I contributed to data acquisition and analysis of the following parts of this publication after familiarization with the technical methods and completion of the animal testing course: I performed the phenotype analysis of PTEC- and DC-activated $CD8^+$ T cells including performance of the co-cultures and analysis by flow cytometry and LEGENDplex as well as viSNE analysis. I further did the phenotype analysis of $CD8^+$ T cells in murine lupus nephritis. Consequently, the experiments that I performed led to the data depicted in figures 3, 4, parts of figure 8, figure S2, S3, S4, and parts of figure S7. For the co-culture of PTECs with OVA-specific $CD8^+$ T cells, I isolated PTECs from the kidneys of naïve mice with the help of Elena Tasika and did the FACS of OVA-specific $CD8^+$ $CD25^-$ T cells shown in figure S2 with the help of the FACS Core Unit. I intraperitoneally injected the WT mice with pristane and took care of these mice for 9 months until analysis. Moreover, I took care of the MRL-*lpr* mice, the *Cd8a*$^{-/-}$ mice and all control mice. From all mice, I regularly collected urine and analyzed the albumin-to-creatinine ratio. For the phenotype analysis of $CD8^+$ T cells after co-culture with PTECs or DCs shown in figures 3, 4, S3, and S4, I harvested the $CD8^+$ T cells and performed the whole staining procedure of cells and subsequent flow cytometry and data analysis. Concerning the lupus nephritis experiments, I carried out the analysis of disease progression, including analysis of lupus-typical autoantibody formation and urinary albumin-to-creatinine ratio. I further isolated renal $CD8^+$ T cells from pristane-treated, MRL-*lpr* and respective control mice and performed the staining of these cells as well as analysis by flow cytometry. Moreover, I revised the manuscript of this publication including supplemental data.

7 Acknowledgements

The opportunity to work on a high-quality experimental medical doctoral thesis as part of the Research Training Group within the SFB1192 “Immune-Mediated Glomerular Diseases – Basic Concepts and Clinical Implications” was an outstanding experience for me, which I would not want to miss. The year in the Research Training Group enabled me to grow both professionally and personally and motivated me to become a clinician scientist. This experience and the successful work on my topic would not have been possible without the help, support and commitment of many others.

Firstly, I thank Prof. Gisa Tiegs who gave me the opportunity to work on my interesting topic in her laboratory. She, together with the whole Research Training Group, enabled me a well-supervised experimental work as well as the opportunity to present and discuss my findings in her lab meetings and above that within the SFB meeting. Moreover, the Research Training Group made it possible for me to take part at the 11th Annual Meeting of the DGfN in Düsseldorf, where I could present my data in a poster session. The seminars trained me for good scientific practice, excellent presentations and scientific writing. At this point, my thank goes to Annett Peters, who organized not only our seminars, but also the application process and the laboratory animal course and was always reachable, when I had questions concerning some laboratory methods.

My thanks further go to Prof. Ulf Panzer for being the second expert on my work and for being part of the supervision committee together with Prof. Oliver Steinmetz. At this point, my thank goes to Prof. Linda Diehl, Prof. Christoph Schramm, Dr. Dorothee Schwinge and Prof. Hans-Willi Mittrücker for providing OT-I mice for my experiments. I further thank Prof. Thorsten Wiech and Dr. Simon Melderis for the pathological scoring of the murine kidney sections of this study.

My special thanks go to Dr. Katrin Neumann, who not only supervised me during the experimental work in the laboratory, but also during the writing of this thesis. Without her support, I would not have come this far. She introduced me to scientific presentations, posters and evaluations, and we had many constructive discussions about the achieved results and how they were placed in the scientific context. I was always able to contribute my own ideas and suggestions.

Above that, Dr. Claudia Wegscheid is an excellent postdoc and always had an open ear for my questions. She, together with Katrin, introduced me to the different methods of laboratory work, flow cytometry and scientific evaluations. If anyone had a question about the practical performance of any laboratory method, Claudia was the one to ask because

she always and immediately had a good idea. I really appreciate the solution-oriented nature of her way of working.

I want to thank Elena Tasika, Carsten Rothkegel and Paulina Sprezyna for the excellent, patient and reliable training in all laboratory equipment, chemicals and methods. Moreover, the entire team contributed to a nice and openhearted working atmosphere and funny, sociable evenings. For this, I would like to thank Prof. Linda Diehl, Dr. Ludmilla Unrau, PD Dr. Andrea Horst, Dr. Aaron Ochel, Dr. Birgit Schiller, Dr. Laura Berkhout, Dr. Gevitah Ananthavettivelu, Mareike Kellerer, Bernd Geers, Selina Wachtendorf, Laura Mayer, Katharina Moll, Charlotte Rumer, and Sebastian Schöls.

Finally, I would like to express my great thanks to my friends and fellow students. I thank my friends Helena, Theresia, Jasmin, Saskia, Anna Maria, and Mareike for our long friendship, our funny evenings and journeys and our deep talks. You were there for me during good and hard times and always motivated me to give my best to become a sensitive and excellent doctor. I further thank my fellow students Eva, Luise, Enikö and Jennie for the great time that we spent together during our medical studies, the professional and personal conversations, our bike travels and the great mutual support.

Last but not least, I want to thank my family with all my heart. My parents, Angela and Burkhard, who laid the foundation for my curiosity for medicine, nature and science and enabled me to study medicine. You encouraged me to question existing values and to build a life corresponding to my own values. And I thank my siblings, Verona and Vincent, with whom I had the most fun from an early age and who have always been behind me. Together as a family, we have mastered all our challenges and experienced the greatest journeys around the globe.

8 Curriculum vitae

Lebenslauf aus datenschutzrechtlichen Gründen nicht enthalten.

Lebenslauf aus datenschutzrechtlichen Gründen nicht enthalten.

9 Eidesstattliche Versicherung

Ich versichere ausdrücklich, dass ich die Arbeit selbständig und ohne fremde Hilfe verfasst, andere als die von mir angegebenen Quellen und Hilfsmittel nicht benutzt und die aus den benutzten Werken wörtlich oder inhaltlich entnommenen Stellen einzeln nach Ausgabe (Auflage und Jahr des Erscheinens), Band und Seite des benutzten Werkes kenntlich gemacht habe.
Ferner versichere ich, dass ich die Dissertation bisher nicht einem Fachvertreter an einer anderen Hochschule zur Überprüfung vorgelegt oder mich anderweitig um Zulassung zur Promotion beworben habe.

Ich erkläre mich einverstanden, dass meine Dissertation vom Dekanat der Medizinischen Fakultät mit einer gängigen Software zur Erkennung von Plagiaten überprüft werden kann.

Unterschrift: .....